Pacific Northwest
NATIONAL LABORATORY

PNNL-30712, Rev. 1
RPT-DFTP-025, Rev. 1

Ion Exchange Processing of AP-105 Hanford Tank Waste through Crystalline Silicotitanate in a Staged 2- then 3-Column System

August 2022

SK Fiskum
AM Westesen
AM Carney
TT Trang-Le
RA Peterson

U.S. DEPARTMENT OF ENERGY

Prepared for the U.S. Department of Energy
under Contract DE-AC05-76RL01830

DISCLAIMER

PACIFIC NORTHWEST NATIONAL LABORATORY
operated by
BATTELLE
for the
UNITED STATES DEPARTMENT OF ENERGY
under Contract DE-AC05-76RL01830

Printed in the United States of America

Available to DOE and DOE contractors from the Office of Scientific and Technical Information,
P.O. Box 62, Oak Ridge, TN 37831-0062
www.osti.gov
ph: (865) 576-8401
fax: (865) 576-5728
email: reports@osti.gov

Available to the public from the National Technical Information Service
5301 Shawnee Rd., Alexandria, VA 22312
ph: (800) 553-NTIS (6847)
or (703) 605-6000
email: info@ntis.gov
Online ordering: http://www.ntis.gov

PNNL-30712, Rev. 1
RPT-DFTP-025, Rev. 1

Ion Exchange Processing of AP-105 Hanford Tank Waste through Crystalline Silicotitanate in a Staged 2- then 3-Column System

August 2022

SK Fiskum
AM Westesen
AM Carney
TT Trang-Le
RA Peterson

Prepared for
the U.S. Department of Energy
under Contract DE-AC05-76RL01830

Pacific Northwest National Laboratory
Richland, Washington 99354

Change History

Revision	Date Issued	Description of Change
0	January 2021	Initial Issue.
1	August 2022	A recent review of RPT-DFTP-025 Rev. 0 resulted in a discovered typo in Table 3.2 characterizing the Cs isotopic ratio in the as-received AP-105. The table incorrectly identified the ^{134}Cs isotope where it should have been ^{135}Cs. The Analytical Service Request, 0964, attached to the report in Appendix C, correctly identified the isotope. The typo has been corrected to the ^{135}Cs isotope and is a minor change that does not affect the report conclusions.

Executive Summary

The Tank Side Cesium Removal (TSCR) system, under development by Washington River Protection Solutions LLC (WRPS), will send initial low-activity Hanford waste tank supernate feeds to the Hanford Waste Treatment and Immobilization Plant (WTP) Low-Activity Waste (LAW) Facility. In addition to entrained solids removal from the supernate, the primary goal of TSCR is to remove cesium-137 (^{137}Cs) by ion exchange, allowing contact handling of the liquid effluent product at the WTP. Crystalline silicotitanate (CST) ion exchange media, manufactured by Honeywell UOP, LLC (product IONSIV™ R9140-B), was selected as the ion exchange media at TSCR.

CST is a non-elutable inorganic material that has demonstrated robust chemical, physical, and radiation tolerance while maintaining functionality. However, exchange kinetics of Cs onto CST is slow, resulting in low utilization of the CST Cs load capacity before unacceptable Cs breakthrough. Two process flow designs have been tested, as follows.

1. Lead-lag column processing: The lead column was removed after the lag column effluent reached the waste acceptance criteria (WAC) limit,[1] the lag column was moved into the lead position, and a new lag column was installed. This format used ~52% Cs load capacity on the lead column.[2]

2. Lead-lag-polish column processing: The processing was stopped when the polish column effluent reached the WAC limit. This format resulted in 81% Cs load capacity on the lead column.[3]

Testing with diluted feed from Hanford tank AP-105 (AP-105DF) incorporated a nuanced change to the lead-lag-polish column system where the polish column was inserted when the lag column effluent reached WAC limit. A 10.9-L volume of AP-105DF (diluted to 5.6 M Na) was processed through the Direct Feed Test Platform system, established at Pacific Northwest National Laboratory to support small-scale waste qualification efforts. The columns consisted of 10-mL CST beds (CST Lot 2002009604, sieved to screen out >30-mesh particles) placed in 1.5-cm-inner-diameter columns. Feed was processed at 1.83 bed volumes (BV) per hour; the flowrate, in terms of contact time with the CST bed, matched the expected flowrate at TSCR. The <30-mesh CST sieve cut was expected to provide appropriate performance scaling to a full-height column. The installation of the polish column later in processing (after processing 523 BVs) did not appear to fundamentally change the utilization of the lead column for Cs exchange nor did it extend the total feed processing volume when compared to the previous test with AP-107 feed.[3] Table ES.1 and Figure ES.1 summarize the measured AP-105DF Cs load performance.

[1] From *ICD 30 – Interface Control Document for Direct LAW Feed*, 24590-WTP-ICD-MG-01-030, Rev. 0, 2015, Bechtel National, Inc. (River Protection Project Waste Treatment Plant), Richland, Washington.
[2] Rovira AM, SK Fiskum, HA Colburn, JR Allred, MR Smoot, and RA Peterson. 2018. *Cesium Ion Exchange Testing Using Crystalline Silicotitanate with Hanford Tank Waste 241-AP-107.* PNNL-27706, RPT-DFTP-011, Rev. 0, Pacific Northwest National Laboratory, Richland, Washington.
[3] Fiskum SK, AM Rovira, HA Colburn, AM Carney and RA Peterson. 2019. *Cesium Ion Exchange Testing Using a Three-Column System with Crystalline Silicotitanate and Hanford Tank Waste 241-AP-107*. PNNL-28958, Rev. 0, RPT-DFTP-013, Rev. 0. Pacific Northwest National Laboratory. Richland, Washington.

Table ES.1. AP-105DF Column Performance Summary with CST

Column	WAC Limit Breakthrough (BVs)	50% Cs Breakthrough (BVs)	^{137}Cs Loaded (µCi/g)	Cs Loaded (mmoles/g CST)
Lead	187	647	86,580	0.0402
Lag	560	1239[(b)]	41,110	0.0191
Polish	974[(a)]	NA	5,370	0.0025

(a) The polish column was positioned in place after 523 BVs were processed through the lead-lag column system.
(b) Extrapolated value.
BV = bed volume, 10 mL
The time weighted average flowrate was 1.83 BV/h.

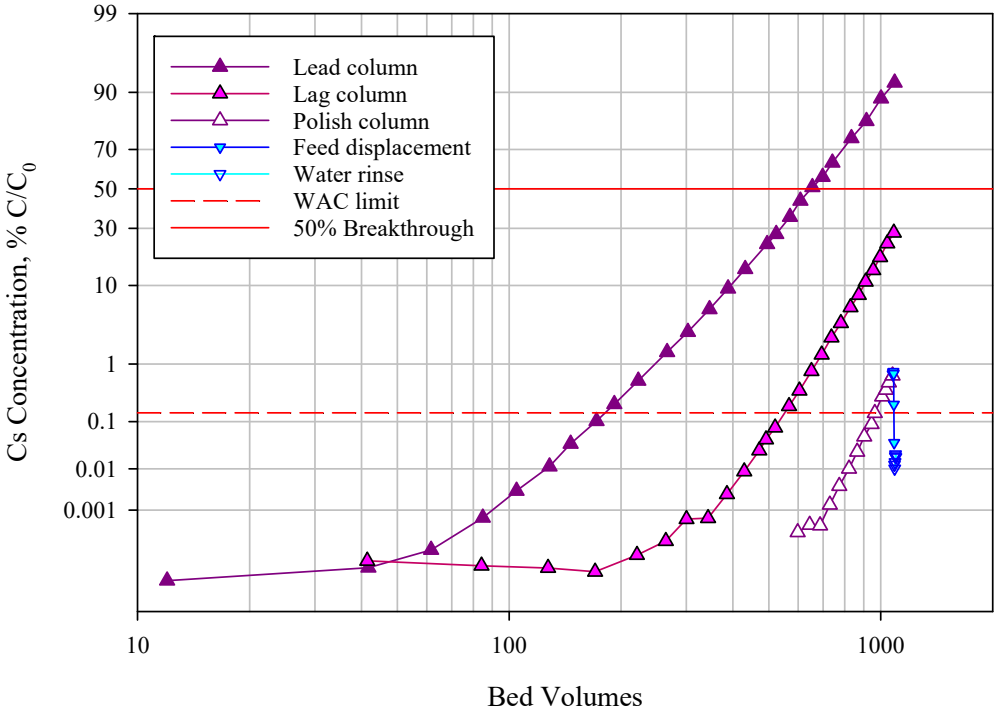

Figure ES.1. Lead, Lag, Polish Column Cs Load Profiles for AP-105DF

Batch contact tests were performed with the AP-105DF tank waste at five Cs concentrations, each at a phase ratio of 200 (liquid volume to dry CST mass). The distribution coefficient (K_d) at the equilibrium condition of 5.66E-5 M Cs (AP-105DF feed condition) was 760 mL AP-105DF/g CST. With a CST bed density of 1.00 g/mL (<30 mesh CST), this K_d corresponded to a predicted 50% Cs breakthrough of 760 BVs. The observed column performance 50% Cs breakthrough (647 BVs) fell ~15% short of the predicted performance (760 BVs). The batch contact testing predicted a Cs load capacity of 0.0420 mmoles Cs/g dry CST at the equilibrium Cs concentration. The Cs breakthrough from the lead column at the end of processing reached 92% C/C_0 and resulted in 0.0402 mmoles Cs/ g CST— 95% of the maximum Cs loading at feed condition based on prediction from batch contact testing.

The AP-105DF composite feed and composite effluent were characterized to understand the fractionation of selected metals and radionuclides. Concentrations and recoveries of the selected analytes are summarized in Table ES.2; those with low recovery were assumed to be adsorbed onto CST. Large fractions of lead (Pb), neptunium (Np), plutonium (Pu), and strontium (Sr/^{90}Sr) significantly fractionated to the CST.

Table ES.2. Recoveries of Analytes of Interest in the AP-105DF Effluent

	Analyte	Feed Concentration (M)	Effluent Concentration (M)	Fraction in Effluent
Metals / Non-metals	Al	5.26E-01	5.23E-01	99%
	As	<5.5E-04	[9.7E-04]	--
	Ba	<1.06E-06	<1.3E-06	--
	Ca	1.03E-03	1.02E-03	99%
	Cd	[2.4E-05]	[2.0E-05]	--
	Cr	6.43E-03	6.56E-03	101%
	Fe	[2.0E-05]	<1.6E-05	--
	K	1.02E-01	1.02E-01	100%
	Na	5.92E+00	6.00E+00	101%
	Nb	2.74E-07	2.89E-05	NA
	P	1.27E-02	1.44E-02	113%
	Pb	9.00E-05	2.67E-05	29%
	S	4.66E-02	4.65E-02	99%
	Sr	1.82E-06	1.64E-07	9%
	Ti	<5.9E-06	[2.3E-05]	NA
	U	2.46E-05	1.99E-05	80%
	Zn	[4.6E-05]	[4.7E-05]	--
	Zr	<9.4E-06	[4.5E-05]	NA
	Analyte	Feed Concentration (μCi/mL)	Effluent Concentration (μCi/mL)	Fraction in Effluent
Radionuclides[(a)]	^{90}Sr	6.90E-01	7.23E-04	0.10%
	^{99}Tc	1.13E-01	1.05E-01	93%
	^{137}Cs	1.13E+02	5.36E-02	0.047%
	^{237}Np	6.69E-06	1.22E-06	18%
	^{238}Pu	6.37E-06	2.64E-06	41%
	$^{239+240}$Pu	3.94E-05	1.56E-05	39%
	^{241}Am	2.66E-04	2.30E-04	86%

(a) Reference date is December 2020.
Notes:
"<" values were < method detection limit (MDL), sample-specific MDL provided.
"--" indicates effluent recovery could/should not be calculated; feed and/or effluent result was < estimated quantitation limit (EQL).
Values in brackets [ ] were ≥ MDL but < EQL, with errors likely to exceed 15%.
NA = not applicable; analytes are CST components
The recovered fractions are calculated with values containing more significant figures than shown; using listed values may result in a slight difference due to rounding.

Acknowledgments

The authors thank Shielded Facility Operations staff Hollan Brown, Victor Aguilar, Jarrod Turner, and Mike Rojas for hot cell operations (batch contact and ion exchange column system setup, processing, and sample removal). We thank the Analytical Support Operations (ASO) staff Karl Pool, Lori Darnell, Jenn Carter, Denis Cherkasov, Sam Morrison, and Andrew Carney for the sample analysis, data processing, and reporting. The authors thank Dr. Heather Colburn and Renee Russell for conducting the technical reviews of the calculation files and this report. The authors also thank Bill Dey for the quality review of the calculation files and this report and Matt Wilburn for his technical editing contribution to this report.

Acronyms and Abbreviations

AEA	alpha energy analysis
ASO	Analytical Support Operations
ASR	Analytical Service Request
BV	bed volume
CST	crystalline silicotitanate
DF	decontamination factor
DI	deionized
EQL	estimated quantitation limit
FD	feed displacement
GEA	gamma energy analysis
IC	ion chromatography
ICP-MS	inductively coupled plasma mass spectrometry
ICP-OES	inductively coupled plasma optical emission spectrometry
ID	identification (number)
LAW	low-activity waste
MDL	method detection limit
ORNL	Oak Ridge National Laboratory
PNNL	Pacific Northwest National Laboratory
PTFE	polytetrafluoroethylene
QA	quality assurance
R&D	research and development
RPD	relative percent difference
RPL	Radiochemical Processing Laboratory
RSD	relative standard deviation
SV	system volume
TIC	total inorganic carbon
TOC	total organic carbon
TRU	transuranic
TSCR	Tank Side Cesium Removal
WAC	waste acceptance criteria
WRPS	Washington River Protection Solutions
WTP	Hanford Waste Treatment and Immobilization Plant
WWFTP	WRPS Waste Form Testing Program

Contents

Figures

Tables

1.0 Introduction

The U.S. Department of Energy (DOE) is working to expedite processing of Hanford tank waste supernate at the Hanford Waste Treatment and Immobilization Plant (WTP). To support this goal, Washington River Protection Solutions, LLC (WRPS, Richland, WA) is designing a system for suspended solids and cesium ($Cs/^{137}Cs$) removal from Hanford tank waste supernate. The effluent will then be sent to the WTP Low-Activity Waste (LAW) Facility for vitrification. The Cs removal is critical for eliminating the high dose rate associated with ^{137}Cs and facilitating a contact maintenance philosophy for the LAW Facility. The maximum ^{137}Cs concentration in the LAW sent to the WTP is targeted to be below the 3.18E-5 Ci ^{137}Cs/mole of Na waste acceptance criteria (WAC) limit.[1] The filtration and ion exchange systems will be placed near the Hanford tanks and are collectively termed the Tank Side Cesium Removal (TSCR) system (Ard 2019).

Crystalline silicotitanate (CST) ion exchange media, product IONSIV™ R9140-B, manufactured by Honeywell UOP, LLC (Des Plaines, IL), was selected as the ion exchange media at the TSCR system. CST is a non-elutable inorganic material that has demonstrated robust chemical, physical, and radiation tolerance while maintaining functionality (Pease et al. 2019). Testing of $^{137}Cs/Cs$ removal from defense wastes using CST has been previously reported (King 2007; Walker et al. 1998; Hendrickson et al. 1996; Brown et al. 1996). Exchange kinetics of Cs onto CST is slow, demonstrated by its long transition zone. The long transition zone challenges full utilization of the CST Cs capacity (Fiskum et al. 2019a). Two column process flow designs have been tested for TSCR on Hanford tank wastes, as follows.

1. **Lead-lag column processing:** The lead column is removed after the lag column effluent reaches the WAC limit and then the lag column is moved up to the lead position and a new lag column is installed (AP-107 tank waste, Rovira et al. 2018, and AW-102 tank waste, Rovira et al. 2019). When processing AP-107 tank waste, 25% Cs breakthrough from the lead column was achieved before it was required to be removed and only partial utilization of the CST bed was achieved. Insufficient volume of AW-102 was available to fully test the Cs loading limits.

2. **Lead-lag-polish column processing:** Feed processing is stopped when the polish column effluent reaches the WAC limit (AP-107 tank waste, Fiskum et al. 2019b). In this case, an extrapolated ~1010 bed volumes (BVs) of feed, corresponding to an estimated 62% Cs breakthrough from the lead column, would have been processed when the WAC limit was reached at the polish column effluent. With the polish column in place, higher lead column utilization was realized.

The primary objective of the work described in this report was to test Cs removal using a hybrid column processing scenario and establish Cs load profiles. In this case, a lead-lag column system was used, and once the lag column effluent reached the WAC limit, a polish column was positioned after the lag column and processing continued. Additional objects of this current study are as follows.

1. Conduct batch contact testing with CST to determine the Cs load capacity of diluted and filtered AP-105 (AP-105DF).

2. Compare the AP-105DF Cs load profile to the previously reported AP-107 load curve (Fiskum et al. 2019b).

[1] From *ICD 30 – Interface Control Document for Direct LAW Feed*, 24590-WTP-ICD-MG-01-030, Rev. 0, 2015, Bechtel National, Inc. (River Protection Project Waste Treatment Plant), Richland, Washington.

3. Analyze the AP-105DF ion exchange feed and effluent to derive the fates of key analytes (^{90}Sr, ^{99}Tc, ^{137}Cs, $^{239+240}$Pu, ^{237}Np, ^{241}Am, Al, As, Ba, Ca, Cd, Cr, Fe, K, Na, Nb, P, Pb, S, Sr, Ti, U, Zn, Zr).

4. Provide Cs-decontaminated AP-105DF for vitrification (to be conducted later and addressed in a separate report).

5. Provide Cs-loaded CST for follow-on analysis (to be conducted later and addressed in a separate report).

The efficacy of loading higher amounts of Cs onto the lead column CST while maintaining a product below the WAC limit from the lag and then polish columns was of prime interest to support the evolving WRPS TSCR design. This test design further exposes the CST to higher feed volume through the individual column beds, allowing for a more representative assessment of the fractionations of analytes of interest.

WRPS funded Pacific Northwest National Laboratory (PNNL) to conduct testing with AP-105DF tank waste under contract 36437/289.

2.0 Quality Assurance

The work described in this report was conducted with funding from WRPS contract 36437/289, *DFLAW Radioactive Waste Test Platform*. This contract was managed under PNNL Project 73312. All research and development (R&D) work at PNNL is performed in accordance with PNNL's Laboratory-Level Quality Management Program, which is based on a graded application of NQA-1-2000, *Quality Assurance Requirements for Nuclear Facility Applications* (ASME 2000), to R&D activities. To ensure that all client quality assurance (QA) expectations were addressed, the QA controls of the PNNL's WRPS Waste Form Testing Program (WWFTP) QA program were also implemented for this work. The WWFTP QA program implements the requirements of NQA-1-2008, *Quality Assurance Requirements for Nuclear Facility Applications* (ASME 2008), and NQA-1a-2009*, Addenda to ASME NQA-1-2008* (ASME 2009), and consists of the WWFTP Quality Assurance Plan (QA-WWFTP-001) and associated QA-NSLW-numbered procedures that provide detailed instructions for implementing NQA-1 requirements for R&D work.

The work described in this report was assigned the technology level "Applied Research" and was planned, performed, documented, and reported in accordance with procedure QA-NSLW-1102, *Scientific Investigation for Applied Research*. All staff members contributing to the work received proper technical and QA training prior to performing quality-affecting work.

3.0 Test Conditions

This section describes the CST media, AP-105DF tank waste, batch contact conditions, and column processing conditions. All testing was conducted in accordance with a test plan prepared by PNNL and approved by WRPS.[1]

3.1 CST Media

WRPS purchased ten 5-gallon buckets (149 kg total) of IONSIV ™ R9140-B[2], Lot number 2002009604, material number 8056202-999, from Honeywell UOP, LLC. This CST production lot was screened by the manufacturer to achieve an 18 × 50 mesh size product. The product was requested to be delivered to WRPS in a series of 5-gallon buckets (as opposed to a 50-gallon drum) to aid in material distribution, handling, and sampling at PNNL. The CST was transferred from WRPS to PNNL on September 20, 2018, under chain of custody. Once received, the CST was maintained at PNNL in environmentally controlled spaces. One of the 5-gallon buckets of CST was delivered to the PNNL Radiochemical Processing Laboratory (RPL). The handling and splitting of the CST were previously described (Fiskum et al. 2019a). A 180-g subsample split was passed through a 30-mesh sieve (ASTM E11 specification) as previously described (Fiskum et al. 2019a). Of this starting mass, 65.6 g or 36 wt% passed through the sieve and was collected for batch contact testing and column testing; this was similar to the 32% mass fraction achieved by Westesen et al. (2020). The <30-mesh CST fraction was pretreated by contacting with 200 mL of 0.1 M NaOH three successive times. The 0.1 M NaOH rinse solution and colloidal fines from the CST were decanted. The rinsed CST was maintained with an overburden of 0.1 M NaOH. Table 3.1 provides the physical properties on <30-mesh sieved CST Lot 2002009604 that had been washed and air dried (Westesen et al. 2020). These properties were expected to apply to the current test because CST processing was essentially identical. The CST particle number across the 1.5-cm column diameter (28) was close to the minimum ideal (≥30) defined by Helfferich (1962) to prevent fluid channeling due to wall effects.

[1] Fiskum SK. 2019. TP-DFTP-076, Rev. 0.0. *Cesium Ion Exchange Testing with AP-105 Tank Waste with Crystalline Silicotitanate for Tank Side Cesium Removal (TSCR)*. Pacific Northwest National Laboratory, Richland Washington. Not publicly available.
[2] R9140-B is provided in the sodium form by the vendor.

Table 3.1. Physical Properties of <30 Mesh CST, Washed R9140-B CST Lot 2002009604 (Westesen et al. 2020)

Parameter	Result	Units
Bulk density	1.03	g/mL
CST bed density	1.00	g/mL
Settled bed void volume	68.2	%
Cumulative particle undersize fractions[(a)]	d_{10}: 398 d_{50}: 541 d_{90}: 738	microns
Column inner diameter	1.5	cm
Particle number across column diameter (based on d_{50})	28	NA

(a) Volume basis, post-sonication

3.2 AP-105DF Tank Waste Sample

Multiple samples (36 each at ~250 mL for a combined ~9 L) were collected in two sets from Hanford tank AP-105 in December 2019. The samples were delivered to PNNL's RPL and placed into the Shielded Analytical Laboratory hot cells. Analytical measurements were conducted by the Analytical Support Operations (ASO) according to two Analytical Service Requests (ASRs); results are provided in Table 3.2. The first sample from the first set, 5AP-19-01, was subsampled and analyzed to confirm Al, K, and Na concentrations by inductively coupled plasma optical emission spectrometry (ICP-OES) (ASR 0957). Subsamples from both the first and last samples from the first set delivered, 5AP-19-01 and 5AP-19-18, were measured for the ^{137}Cs concentration by gamma energy analysis (GEA) (ASR 0957). Following Cs separation, the Cs isotopic ratio was measured by inductively coupled plasma mass spectrometry (ICP-MS) (ASR 0964). The AP-105 densities were measured in-cell using 10-mL volumetric flasks. The results of the duplicate pairs agreed within 4% relative percent difference (RPD), it was assumed that all 36 samples were essentially homogenous, within analytical uncertainty (±10% to 15%).

Table 3.2. Characterization of Samples 5AP-19-01 and 5AP-19-18 Collected from Hanford Tank AP-105 December 2019 (ASR 0957, 0964)

Sample ID>>	5AP-19-01	5AP-19-18	5AP-19-25			
RPL Number>>	20-0321	20-0322	NA			
Analyte				RPD, %	Units	Analysis Method
Al	7.86E-01	--	--	--	M	ICP-OES
K	1.71E-01	--	--	--	M	ICP-OES
Na	8.72E+00	--	--	--	M	ICP-OES
^{137}Cs[(a)]	193	186	--	3.8	µCi/mL	GEA
RPL Number>>	20-0350	20-0351	NA			
^{133}Cs	62.3	61.8	--	0.93	Wt%	ICP-MS
^{135}Cs	19.5	19.5	--	0.08	Wt%	ICP-MS
^{137}Cs[(a)]	18.2	18.7	--	3.0	Wt%	ICP-MS
Density	1.414	--	1.412	0.1	g/mL	Volumetric flask

(a) Reference date is 12/17/19.

The AP-105 tank waste samples were composited and diluted in stages to achieve a 5.92 M Na concentration as previously described (Allred et al. 2020). Nominally three samples were combined into a polyethylene bottle and Columbia River process water was added. The AP-105 and water were mixed and allowed to stand for 3 to 6 months before filtration testing. After filtration, 10 bottles of AP-105 diluted feed (AP-105DF), containing 0.9 to 1.3 L each, were made available for ion exchange testing.

The densities and ^{137}Cs concentrations of each of the 10 bottles of AP-105DF were measured. The density average was 1.285 g/mL [0.38% relative standard deviation (RSD)] and the ^{137}Cs average was 121.7 µCi/mL (1.8% RSD; reference date June 2020). Therefore, AP-105DF feeds in all containers were considered uniform. The total Cs concentration was calculated from the ^{137}Cs concentration (in terms of µg/mL with unit conversion per the specific activity) and ^{137}Cs mass fraction (average 18.5 wt%). The total Cs concentration in the AP-105DF was 7.58 µg/mL or 5.66E-5 M. This value agreed within 5% of the total Cs concentration, 7.92 µg/mL (reference date August 9, 2017), reported previously for AP-105 diluted tank waste (Fiskum et al. 2018a).

3.3 Batch Contact Conditions

The distribution coefficient (K_d) is a quantitative measure of a material's capability to remove an ion from a specific solution matrix. Specifically, it is the ratio of analyte ion remaining in solution at equilibrium to the amount of analyte ion sorbed on the ion exchange material. The distribution coefficient is determined from batch contact testing.

Batch contact solutions consisted of AP-105DF tank waste samples plus various amounts of added ^{133}Cs as $CsNO_3$ solution. The equilibrium Cs concentrations were determined after batch contacts to assess the effective Cs loading capacity on the CST and the Cs K_d in the AP-105DF feed matrix. The preparation and batch contacts were processed in accordance with a test instruction.[1]

Aliquots of Cs spike solutions (133 mg/mL or 16.2 mg/mL) were added to four centrifuge tubes in small volumes. The centrifuge tubes with Cs-spike were transferred to the hot cell and ~30-mL aliquots of AP-

[1] Fiskum SK. 2019. TI-DFTP-081, *Batch Contact Testing of Diluted and Filtered AP-105 Hanford Tank Waste with Crystalline Silicotitanate*. Pacific Northwest National Laboratory, Richland, Washington. Not publicly available. Implemented July 2020.

105DF were transferred to each container. Exact masses transferred were determined by difference from the measured masses before and after Cs spikes and AP-105DF transfers; the added volumes were calculated from the solution densities and net sample masses. The four vessels of AP-105DF plus added Cs and the unspiked AP-105DF are termed "stock contact solutions." The stock contact solutions were shaken to mix AP-105DF thoroughly with the Cs spike. Table 3.3 shows the added spiked Cs masses and calculated starting Cs concentrations in the stock contact solutions. The Cs spike solutions were equilibrated with AP-105DF matrix 1 to 2 days.

Table 3.3. Cs Concentrations in Stock Contact Solutions

Solution ID	Added Cs (mg)	Cs Concentration (mg/L)	Cs Concentration (M)
TI081-S0	0	7.58	5.66E-5
TI081-S1	0.808	35.3	2.66E-4
TI081-S2	4.13	150	1.13E-3
TI081-S3	16.11	557	4.19E-3
TI081-S4	58.68	1947	1.47E-2

An aliquot of the washed CST, sufficient to apply to all batch contact tests, was allowed to air-dry overnight at ambient temperature to a free-flowing form. However, the air-dried CST still contained moisture. The F-factor, ratio of dry mass exchanger to sampled mass exchanger, was determined to correct for water content. A small fraction of the air-dried CST was removed for nominal F-factor evaluation. This F-factor sample aliquot was dried at ~103 °C overnight to determine the nominal water content remaining in the air-dried CST. This nominal F-factor was used to determine the target CST aliquot masses to collect for the batch contact samples. The air-dried CST contained ~10% water by mass.

Precisely weighed quantities of the washed and air-dried CST (targeted to be 0.084 g "wet" and 0.075 g dry) were aliquoted into 20-mL liquid scintillation vials, one for each batch contact sample. The air-dried CST mass was determined to an uncertainty of ≤1%.

Two nominal 0.3-g F-factor samples were also collected and precisely weighed, one at the beginning of CST aliquoting process, and one at the end of CST aliquoting process in a tight subsampling time window (≤10 min). The initial F-factor sample masses were designated M_I. The F-factor samples were dried to constant mass at 103 °C. The final F-factor sample masses were designated M_F. The F-factors were calculated according to Eq. (3.1). The average of the two F-factor samples (first and last from the weighing series, 0.8702 ±0.10% RPD) was used to calculate the dry CST masses contacted with AP-105DF.

$$\frac{M_F}{M_I} = F \tag{3.1}$$

The CST aliquots were transferred to the hot cell and then contacted with 15 mL of the various stock contact solutions (see Table 3.3) in duplicate. The AP-105DF volume was transferred by pipet, and the actual volume delivered was determined by mass difference and solution density. The targeted phase ratio (liquid volume to dry exchanger mass) was 200 mL/g CST. The obtained ratio varied between 182 and 207 mL/g CST. The actual batch contacted sample solution volumes and CST masses are shown in Table 3.4.

Table 3.4. Dry CST Masses and AP-105DF Tank Waste Volumes for Batch Contacts

Sample ID	Dry CST Mass[(a)] (g)	AP-105DF Volume (mL)	Liquid-to-Solid Phase Ratio (mL/g)
TI081-S0-BC	0.0764	14.9082	195
TI081-S1-BC	0.0768	14.9221	194
TI081-S2-BC	0.0720	14.9076	207
TI081-S3-BC	0.0730	14.8603	204
TI081-S4-BC	0.0752	14.8888	198
TI081-S0-BC-d	0.0728	13.8412	190
TI081-S1-BC-d	0.0768	13.9652	182
TI081-S2-BC-d	0.0742	13.8748	187
TI081-S3-BC-d	0.0722	14.1719	196
TI081-S4-BC-d	0.0745	14.8689	200

(a) Mass-corrected for water loss at 103 °C.

Four batch contact vials along with a temperature sentinel vial (15 mL of deionized [DI] water) were placed upright onto a Thermo LP vortex mixer[1] set to ~400 revolutions per minute. Agitation continued for 72 h, which had been previously established to reach Cs equilibrium conditions (Fiskum et al. 2019b). The process was repeated for another set of four batch contact vials, and then again for the final two batch contact vials. The average sentinel temperature upon completion of batch contact testing was 29.9 °C with a range of 0.5 °C (Type K thermocouple, accuracy ±2.2 °C). The contact temperature was ~2 °C higher than the ambient cell temperature. No obvious cloudiness was observed in the contact solutions post-processing.

After the batch contact time, the CST was settled and ~ 5 mL of each aqueous fraction was removed from the hot cell. Each sample was filtered through a 0.45-µm pore size nylon-membrane syringe filter. Filtered sample aliquots (2 mL) were collected for gamma counting; the sampled aliquot masses were measured, and the exact volumes determined by dividing by the solution density.

Aliquots of the AP-105DF stock solutions and batch contacted samples were analyzed by gamma spectrometry to determine ^{137}Cs concentrations. The batch contact Cs K_d value was determined for each sample using the relationship shown in Eq. (3.2):

$$\frac{(C_0 - C_1)}{C_1} \times \frac{V}{M \times F} = K_d \quad (3.2)$$

where:

C_0 = initial ^{137}Cs concentration (µCi/mL) in the stock contact solution
C_1 = final ^{137}Cs concentration (µCi/mL) in the batch contacted solution
V = volume of the batch contact liquid (mL)
M = measured mass CST (g)
F = F-factor, mass of the dried CST divided by the mass of the sampled CST
K_d = batch-distribution coefficient (mL/g)

[1] The Thermo LP vortex mixer was selected for hot cell use because of its small size (15.4 x 21.0 x 8.3 cm) and small mass (3.1 kg).

Final Cs concentrations (Cs_F) were calculated relative to the ^{137}Cs recovered in the batch contacted samples according to Eq. (3.3):

$$Cs_0 \times \left(\frac{C_1}{C_0}\right) = Cs_F \quad (3.3)$$

where:

Cs_0 = initial Cs concentration in solution (µg/mL or M)
Cs_F = final Cs concentration in solution (µg/mL or M)

The equilibrium Cs concentrations loaded onto the CST (Cs_{IX} in units of mg Cs per g of dry CST mass) were calculated according to Eq. (3.4):

$$\frac{Cs_0 \times V \times \left(1 - \frac{C_1}{C_0}\right)}{M \times F \times 1000} = Cs_{IX} \quad (3.4)$$

where:

Cs_{IX} = equilibrium Cs concentration in the CST (mg Cs/g CST)
1000 = conversion factor to convert µg to mg

The Cs_{IX} value was divided by the Cs formula weight to determine Q, mmoles analyte/g dry CST. In the case of unspiked AP-105DF, the calculated Cs formula weight of 134 g/mole was applied. For the spiked Cs samples, where natural Cs dominated the isotopic composition, the Cs formula weight of 132.9 g/mole was applied.

The theoretical 50% Cs breakthrough on the ion exchange column (λ) can be predicted from the product of the K_d value and the ion exchanger bed density (ρ_b) according to Eq. (3.5) (Bray et al. 1993). The CST bed density is the dry CST mass divided by the volume in the column:

$$K_d \times \rho_b = \lambda \quad (3.5)$$

3.4 Ion Exchange Process Testing

This section describes the ion exchange column system and AP-105DF process conditions. The preparations and column testing were conducted in accordance with a test instruction.[1]

3.4.1 Ion Exchange Column System

Figure 3.1 provides a schematic of the lead-lag column ion exchange process system; Figure 3.2 shows the lead-lag-polish column configuration schematic. Figure 3.3 shows a photograph of the system before installation in the hot cell. Flow through the system was controlled with a Fluid Metering Inc. (FMI) positive displacement pump. Fluid was pumped past an Ashcroft pressure gage and a Swagelok pressure relief valve (back of manifold) with a 10-psi trigger point. The 1/8-inch outside diameter / 1⁄16-inch inside diameter polyethylene tubing was purchased from Polyconn (Plymouth, MN). The 1/8-inch outside diameter / 1/16-inch inside diameter stainless steel tubing was used in conjunction with the manifold.

[1] Fiskum, SK. 2019. *Cesium Removal from AP-105 Using Crystalline Silicotitanate in a Two and Three-Column Format.* TI-DFTP-082. Pacific Northwest National Laboratory, Richland, Washington. Not publicly available. Implemented July 2020.

Valved quick disconnects were purchased from Cole Parmer (Vernon Hills, IL). Use of the quick disconnects enabled easy disassembly and re-assembly for installation in the hot cell. Multiple quick disconnects were used such that columns could be isolated (required for system install and reserved polish column) or replaced as needed. Also, recovery from upset conditions could be accommodated by allowing access to a column either downflow or upflow.

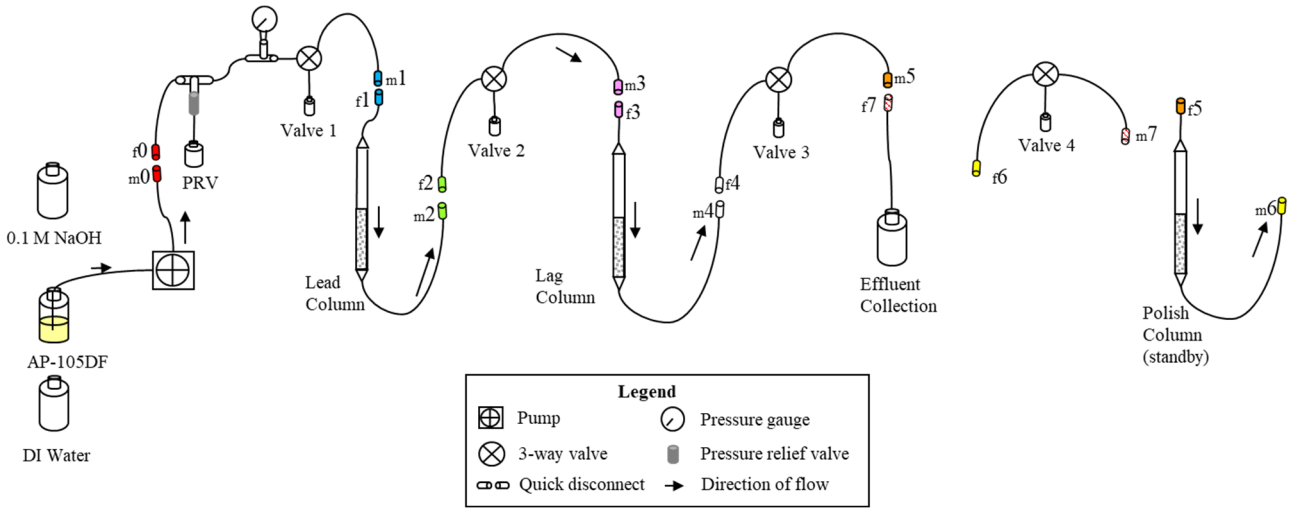

Figure 3.1. Ion Exchange System Schematic (2-Column Configuration)

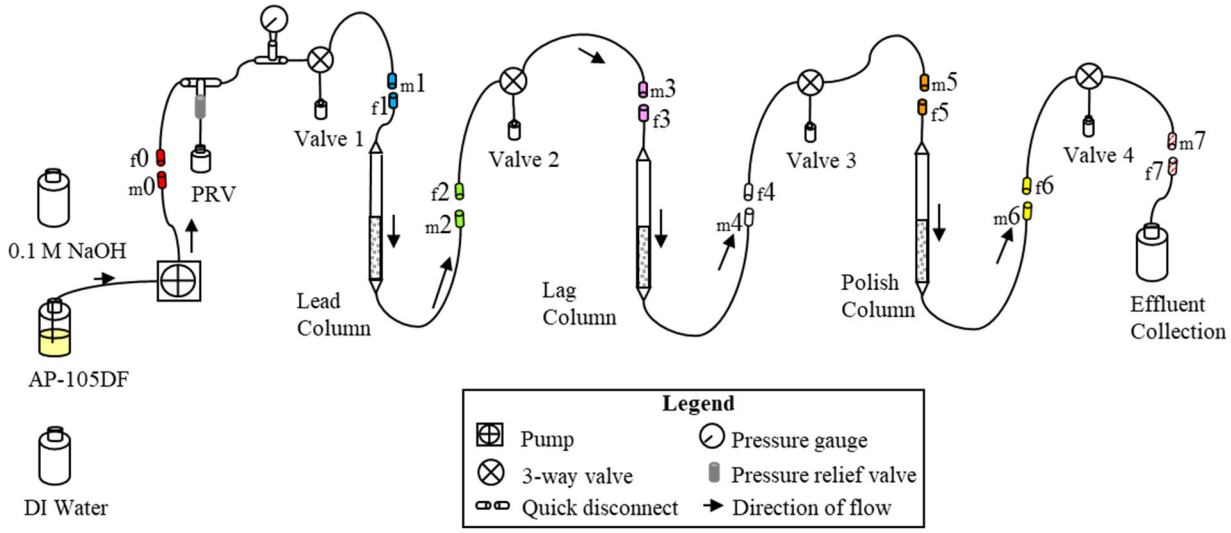

Figure 3.2. Ion Exchange System Schematic (3-Column Configuration)

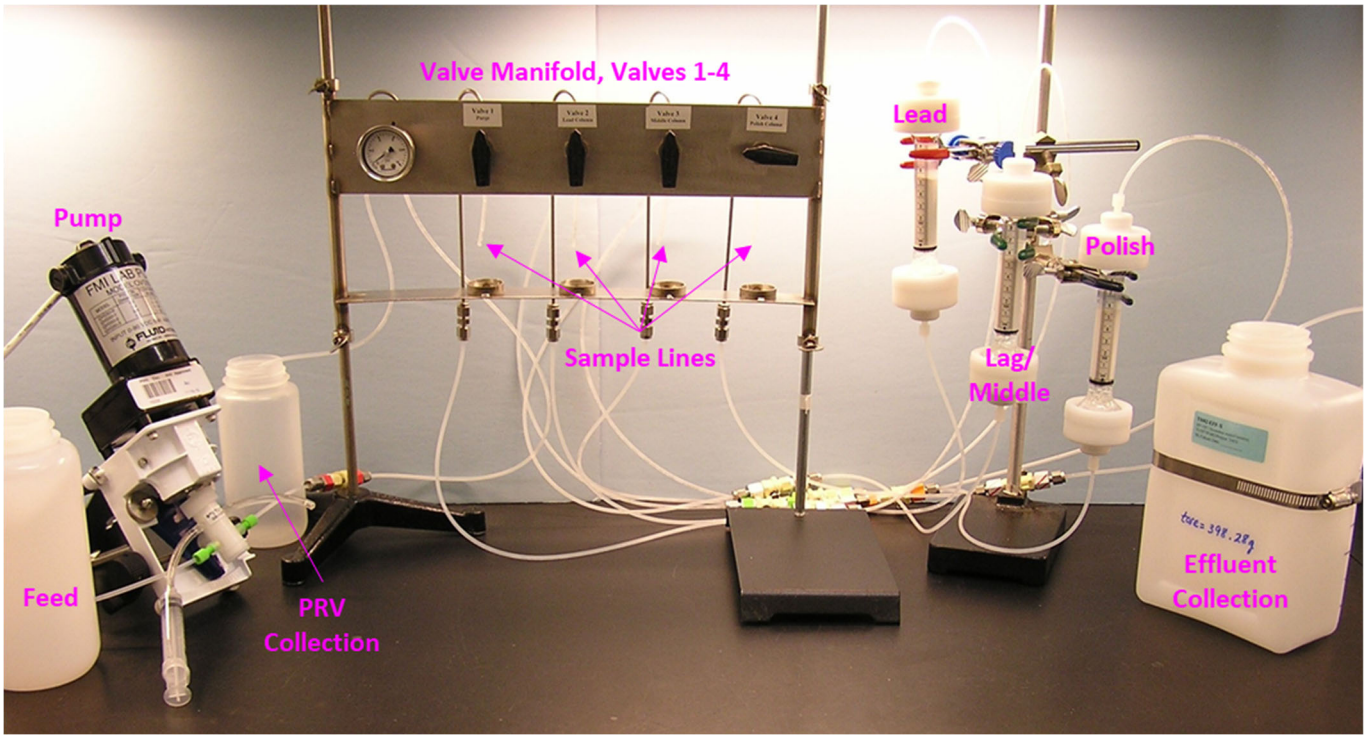

Figure 3.3. Photograph of Ion Exchange System Outside of the Hot Cell

Chromaflex® column assemblies were custom ordered from Kimble Chase (www.kimble-chase.com). Each column assembly included the column plus the standard top and bottom end fittings. Each column was made of borosilicate glass; the straight portion of the column was 9 cm tall with an inside diameter of 1.5 cm (corresponding to a CST volume of 1.77 mL/cm). The 1.5-cm inside diameter columns are not commercial-off-the-shelf items. The columns are flared at each end to support the off-the-shelf column fittings and tubing connectors that were composed of polytetrafluoroethylene (PTFE). The CST was supported by an in-house constructed support consisting of a 200-mesh stainless steel screen tack welded onto a stainless-steel O-ring. With a rubber O-ring, the fitting was snug fitted into place in the column (as previously described by Fiskum et al. 2018b). After packing with CST, a small number of CST particles were observed to have slipped into the narrow gap between the stainless-steel support and glass column barrel; they were blocked from passage by the O-ring. The flared cavity at the bottom of each column was filled to the extent possible with 4-mm-diameter glass beads to minimize the mixing volume below the CST bed. An adhesive centimeter scale with 1-mm divisions (Oregon Rule Co. Oregon City, OR) was affixed to the column with the 0-point coincident with the top of the support screen.

Four Swagelok valves were installed in the valve manifold. Valve 1 was used to isolate the columns from the pump (when in the closed position) and purge the tubing from the inlet to valve 1 (when placed in the sampling position). Lead column samples were collected at valve 2, the lag column samples were collected at valve 3, and the polish column samples were collected at valve 4. The gross AP-105DF effluent, feed displacement (FD), water rinse, and flushed fluid were collected at the effluent line.

The system was filled with water and then slightly pressurized to confirm system leak tightness. The pressure relief valve was confirmed to trigger at the manufacturer set point (10 psig). Water was removed from the columns and replaced with 0.1 M NaOH. Three 10.0-mL aliquots of settled CST (pretreated, <30 mesh) were measured using a graduated cylinder and then quantitatively transferred, one aliquot each, to the three columns. The CST was allowed to settle through the 0.1 M NaOH solution, thus

mitigating gas bubble entrainment. The columns were tapped with a rubber bung until the CST height no longer changed.

The CST BV corresponded to the settled CST media volume as measured in the graduated cylinder prior to transferring the media into the ion exchange column. The reference CST BV was 10.0 mL; each of the three columns contained 10.0 mL CST. The settled CST bed heights in the columns were nominally 5.6 cm. This small column bed height corresponded to 2.4% of the full height column (234 cm or 92 inches) and the BV corresponded to 0.0017% of the full-scale column (596 L) (Siewert 2019).

Figure 3.4 provides a closeup image of the lag column loaded with CST, the fluid headspace, the CST bed support/O-ring, and glass beads filling the void space below the bed. Note that the centimeter scale 0-point is positioned at the CST support screen and some CST particles slipped into the small gap between the column wall and the rubber screen support ring.

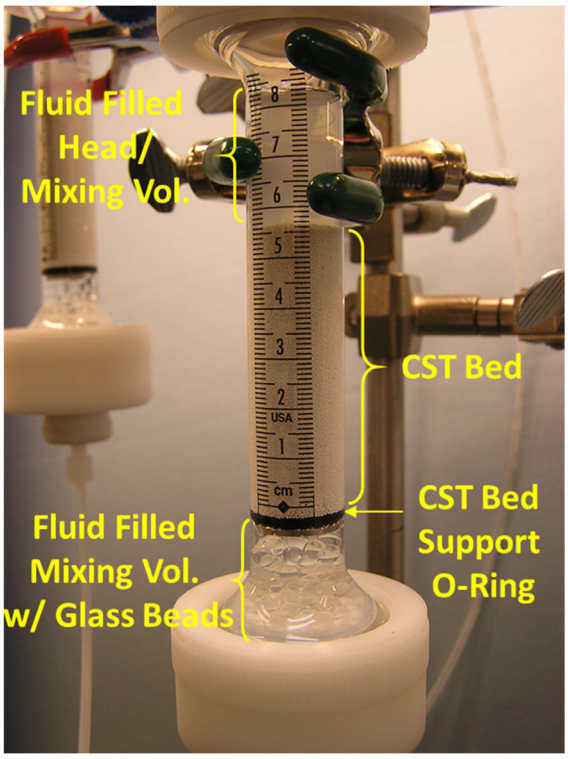

Figure 3.4. Closeup of Lag Chromaflex® Column Loaded with CST

The entire fluid-filled volume of the assembly was calculated for the 2-column system at ~46 mL, and for the 3-column system at ~66 mL. The bed void volume was assigned 66% (Westesen et al. 2020). Therefore, each CST bed held 6.6 mL fluid and the CST beds only comprised ~30% of the fluid-filled volume. The TSCR system platform may have a much larger fluid fraction associated with the CST bed. The fluid-filled mixing space above each CST bed ranged from 3.4 to 4.7 mL. The fluid mixing volume below each CST bed ranged from 2.8 to 3.4 mL. Thus, ~60% of the total fluid holdup volume was unavoidably associated with the geometry of the two and three columns. These scales of fluid mixing volume fractions are not likely to be representative of plant-scale operations.

Figure 3.5 is a photograph of the ion exchange system during in-cell AP-105DF processing approximately 1 week after starting the run.

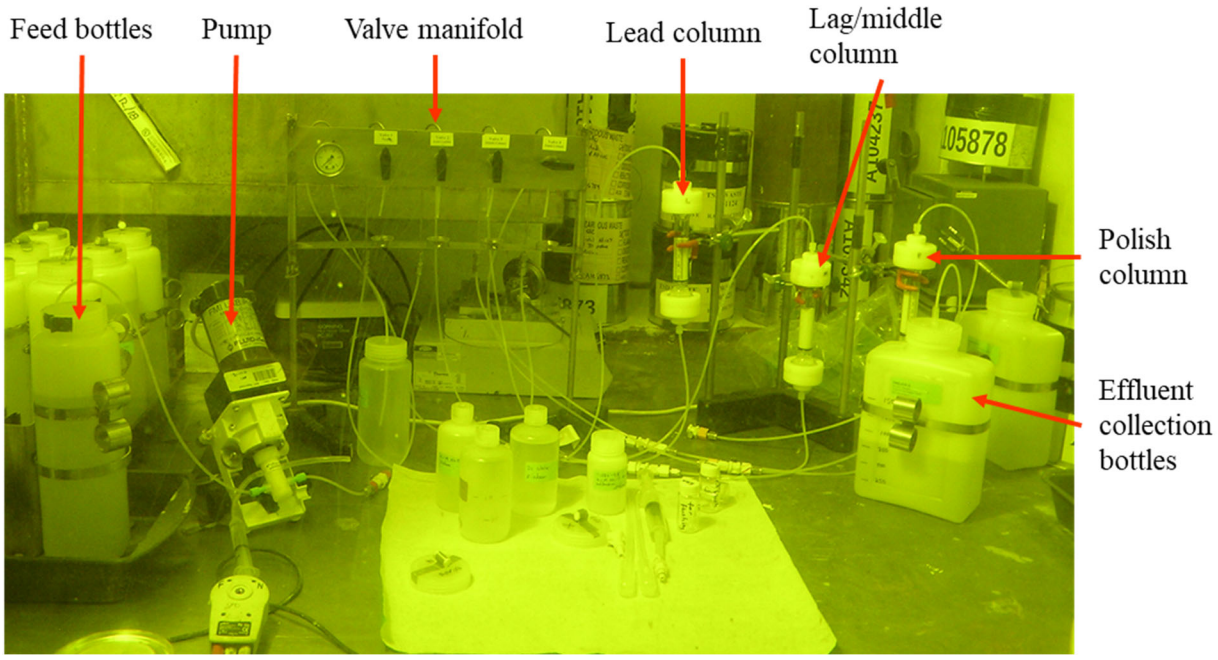

Figure 3.5. Ion Exchange Assembly in the Hot Cell, ~1 Week after Start

3.4.2 AP-105DF Tank Waste Process Conditions

Once the ion exchange assembly was installed in the hot cell, a flow of 0.1 M NaOH was used to verify system integrity and calibrate the pump. The various 1.5-L polyethylene containers from the filtration process (Allred et al. 2020) were used as the ion exchange feed bottles. They were positioned in a bottle stand to provide stability just before the feed line was inserted. When the contents in a feed bottle decreased to ~200 mL, the next bottle in line was moved to the feed position and the residual contents were poured into the new feed bottle. The AP-105DF feed was processed downflow through the ion exchange media beds, lead to lag. Effluent was collected in ~1.0- to 1.3-L increments. The volume limitation allowed for safe transfer out of cell in 1.5-L polyethylene bottles. The lag column effluent Cs concentration was closely monitored. When the WAC limit was reached, the polish column was placed in-line and the run continued.

After the AP-105DF loading was completed, 11 BVs of 0.1 M NaOH FD followed by 11 BVs of DI water were passed downflow through the system to rinse residual feed out of the columns and process lines. The 11 BVs was equivalent to ~1.7 times the fluid-filled system volume (SV).

All processing was conducted at ambient cell temperature, nominally 27 to 29 °C. Test parameters, including process volumes, flowrates, and CST contact times, are summarized in Table 3.5. The pump head stroke length was close to the minimum at which it could be set. The stroke rate was toggled between 12.9 and 13.0 (maximum fidelity of 0.1 units) to maintain the flowrate between 1.8 and 2.0 BV/h, respectively. Greater fidelity with the stroke rate controller could not be obtained to center on the target 1.83 BV/h. Figure 3.6 shows the achieved flowrate as a function of time.

Table 3.5. Experimental Conditions for AP-105DF Column Processing, July 6 to July 31, 2020

		Volume			Flowrate		Duration
Process Step	Solution	(BV)	(SV)	(mL)	(BV/h)	(mL/min)	(h)
Loading lead column	AP-105DF	1091	NA	10906	1.83	0.305	600
Loading lag column[(a)]	AP-105DF	1085	NA	10850	1.83	0.305	600
Loading polish column[(b)]	AP-105DF	516	NA	5161	1.83	0.305	264
Feed displacement	0.1 M NaOH	10.8	1.63	108	2.93	0.489	3.7
Water rinse	DI water	11.2	1.69	112	2.89	0.482	3.9
Flush with compressed air[(c)]	NA	5.2	0.82	52.3	NA	NA	NA

(a) The feed volume through the lag column was reduced relative to that of the lead column because samples collected from the lead column did not enter the lag column.
(b) The feed volume through the polish column was lower relative to that of the lead and lag columns because it was placed in position after 523 BVs were processed.
(c) The flush occurred on August 3, 2020, after the system sat in static contact with water rinse for 66 h (over the weekend).
BV = bed volume (10.0 mL as measured in graduated cylinder).
SV = system volume (estimated 66 mL).
NA = not applicable.

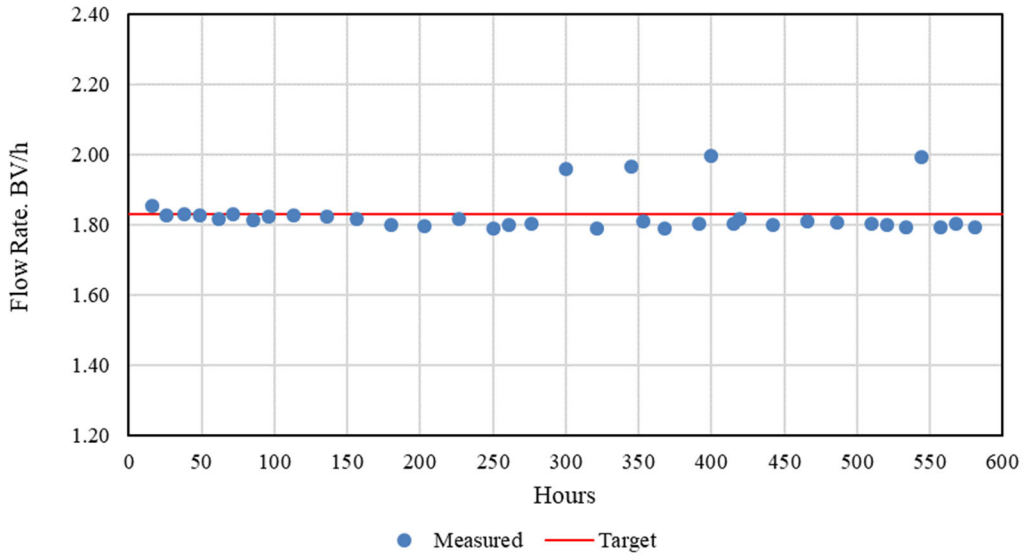

Figure 3.6. AP-105DF Flowrate as a Function of Time

The total cumulative volume of AP-105DF processed was 10.91 L (1091 BVs). The AP-105DF process cycle mimicked, as best as possible, the current process flow anticipated at the TSCR facility in terms of BV/h (i.e., contact time), FD, and water rinse as defined in the test plan. It was understood that the feed linear flow velocity in this small-column configuration (0.17 cm/min) could not begin to match that of the full-height processing configuration (7.3 cm/min, Fiskum et al. 2019a). The point was to match contact time in the bed.

During the loading phase, nominal 2-mL samples were collected from the lead, lag, and polish columns at the sample collection ports (see Figure 3.1, valves 2, 3, and 4). Sampling from the columns necessitated brief (~7-minute) interruptions of flow to the downstream columns. Samples were collected after the first 12 BVs were processed and again at nominal 18- to 93-BV increments. Only brief (~5 min) interruptions were associated with changing the feed bottles.

The FD effluent was collected in a series of 6 vials in ~18-mL increments. The water rinse was similarly collected. The fluid-filled volume was expelled with compressed air connected at the first quick disconnect in the system *f0* (see Figure 3.1) in ~4 min. The collected volume (52.3 mL) did include the interstitial fluid space between the CST beads, but was not expected to include fluid in the CST pore space. Hours of additional gas flow were required to dry the CST enough to be free-flowing such that it would effectively pour out of the columns into specially designed shielded containment for later examination (not addressed in this report). The recovered CST was 10.02 g, 10.28 g, and 10.38 g for the lead, lag, and polish columns, respectively. With a CST bed density is 1.00 g/mL, essentially quantitative recovery of the CST from the columns was estimated.

After setting a couple of days, solids were observed in the flushed solution. The aqueous phase was decanted and removed from the hot cell. The slurry with he settled residual solids was set aside to dry. Some solids were also later found in the decanted solution and are pictured in Figure 3.7. They have the appearance of FeOOH flocculant solids. The dried residue in the parent bottle weighed only 0.026 g; these solids were submitted for acid digestion and ICP-OES analysis per ASR 1109. Solids in gas flushed fluid had not previously been noted; the solids noted herein appeared to be an anomaly.

Figure 3.7. Decanted Flushed Solution Post Water Rinse Showing Settled Solids

3.5 Sample Analysis

Cesium load performance was determined from the ^{137}Cs measured in the collected samples relative to the native ^{137}Cs in AP-105DF feed. The collected samples were analyzed directly to determine the ^{137}Cs concentration using GEA. Cesium loading breakthrough curves for both the lead and lag columns were generated based on the feed ^{137}Cs concentration (C_0) and the effluent Cs concentration (C) in terms of % C/C_0.

A composite feed sample was prepared by sampling 1 mL from each filtered sample bottle into one polyethylene vial. An effluent composite sample was generated by collecting a pro-rated volume from each effluent bottle and combining in a polyethylene vial. Selected effluent samples from the lead column were measured for selected radionuclides and cations in an effort to assess the exchange behavior for these analytes. Table 3.6 summarizes the specific sample collections and targeted analytes along with the cross references to the ASO sample identification numbers (IDs).

The feed and effluent samples were submitted to the ASO on ASR 1097. The ASO was responsible for the preparation and analysis of appropriate analytical batch and instrument quality control samples and for providing any additional processing to the sub-samples that might be required (e.g., acid digestion, radiochemical separations, dilutions). All analyses were conducted by the ASO according to standard operating procedures, the ASO QA Plan, and the ASR. Samples were analyzed directly (no preparation) by GEA, longer count times were used to assess isotopes other than ^{137}Cs.

Table 3.6. Analytical Scope Supporting Column Processing, ASR 1097

Sample ID	ASO Sample ID	Analysis Scope
TI082-COMP-FEED	20-1677	GEA (^{60}Co, ^{137}Cs, ^{154}Eu) ICP-OES (Al, As, Ca, Cd, Cr, Fe, K, Na, P, Si, Ti, Zn, Zr) ICP-MS (Ba, Nb, Pb, Sr, ^{238}U) Radioanalytical (^{90}Sr, ^{99}Tc, ^{237}Np, ^{238}Pu, $^{239+240}$Pu, ^{241}Am)
TI082-COMP-EFF	20-1678	GEA (^{60}Co, ^{137}Cs, ^{154}Eu) IC anions (F^-, Cl^-, NO_2^-, NO_3^-, PO_4^{3-}, $C_2O_4^{2-}$, SO_4^{2-}) Furnace oxidation (TOC, TIC) Acid titration (free OH) ICP-OES (Al, As, Ca, Cd, Cr, Fe, K, Na, P, Si, Ti, Zn, Zr) ICP-MS (Ba, Nb, Pb, Sr, ^{238}U) Radioanalytical (^{90}Sr, ^{99}Tc, ^{237}Np, ^{238}Pu, $^{239+240}$Pu, ^{241}Am)
TI082-L-F2-A	20-1679	ICP-OES (Al, Ca, Cd, Fe, K) ICP-MS (Ba, Pb, ^{238}U) Radioanalytical (^{90}Sr, ^{237}Np, $^{239+240}$Pu)
TI082-L-F4-A	20-1680	
TI082-L-F6-A	20-1681	
TI082-L-F8-A	20-1682	
TI082-L-F10-A	20-1683	
TI082-L-F12-A	20-1684	
TI082-L-F14-A	20-1685	
TI082-L-F16-A	20-1686	
TI082-L-F22-A	20-1687	
TI082-L-F26-A	20-1688	

IC = ion chromatography
TIC = total inorganic carbon
TOC = total organic carbon

4.0 Batch Contact Results

This section discusses the batch contact results for the AP-105DF filtered tank waste with <30-mesh CST Lot 2002009604.

Equilibrium Cs concentrations and K_d results for the batch contacted samples are provided in Table 4.1. The K_d values versus Cs concentrations are plotted in Figure 4.1 on a log-log scale; the AP-105DF Cs concentration is shown in a vertical dashed line. Between 1.6 and 35 µg/mL Cs, the K_d values were essentially constant (flattened portion of the curve). The K_d at the feed condition Cs concentration (7.58 µg/mL) is 760 mL/g. At a bed density of 1.00 g CST/mL, the λ value (K_d x bed density) is therefore predicted to be at ~760 BVs. This value was 7% lower than that predicted for AP-107, 814 BVs at a slightly higher Cs feed concentration of 9.19 µg/mL Cs (Fiskum et al. 2019b).

Table 4.1. Equilibrium Results for AP-105DF Batch Contact Samples with CST Lot 2002009604

Sample ID	Final [Cs] (µg/mL)	Final [Cs] (M)	K_d (mL/g)	Q, Equilibrium Cs in CST (mmoles/g)
TI081-S0-BC	1.64	1.22E-5	706	8.65E-3
TI081-S0-BC-d	1.57	1.17E-5	723	8.52E-3
TI081-S1-BC	7.16	5.39E-5	761	4.11E-2
TI081-S1-BC-d	6.77	5.09E-5	763	3.90E-2
TI081-S2-BC	34.7	2.61E-4	689	1.80E-1
TI081-S2-BC-d	30.8	2.31E-4	725	1.68E-1
TI081-S3-BC	214	1.61E-3	325	5.25E-1
TI081-S3-BC-d	215	1.62E-3	311	5.05E-1
TI081-S4-BC	1371	1.03E-2	83	8.59E-1
TI081-S4-BC-d	1420	1.07E-2	74	7.92E-1

Note that the AP-105DF tank waste constituents also included 0.102 M K and 1.24 M free hydroxide.
Contact time = 72 h
Contact temperature = 30 °C
See Table 3.3 for initial Cs concentrations.
See Table 3.4 for CST masses and contact solution volumes.

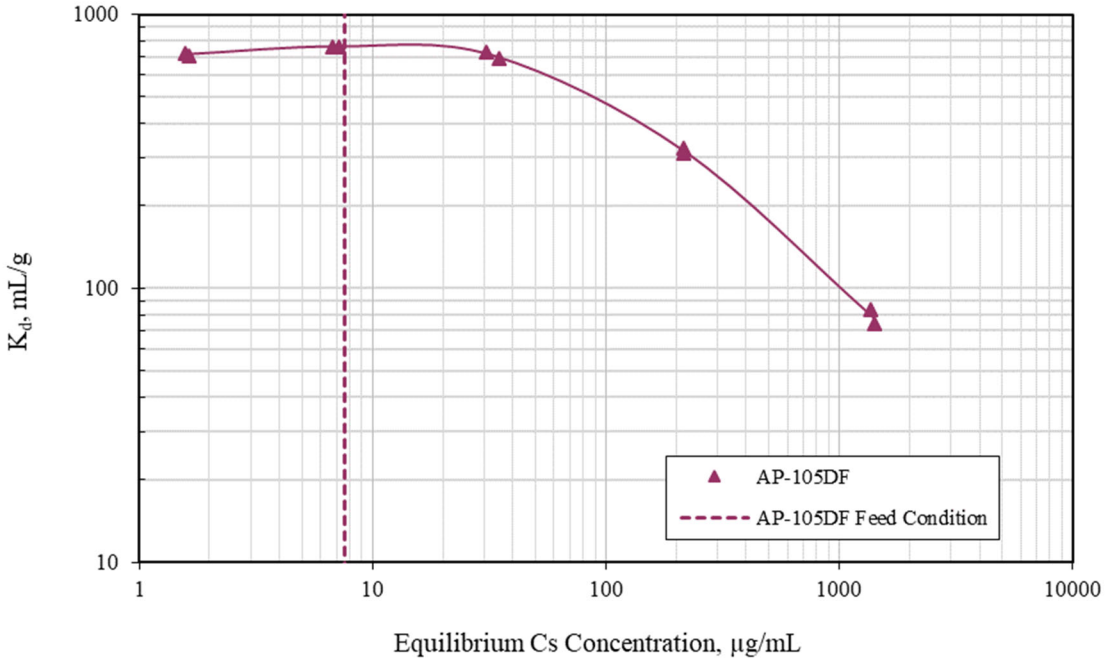

Figure 4.1. Equilibrium Cs K_d Curve for AP-105DF with CST Lot 2002009604

Figure 4.2 provides the isotherms for the AP-105DF batch contact test samples with CST. In this case, the abscissa equilibrium Cs concentration is expressed in terms of molarity and the ordinate is expressed in terms of Q (mmoles Cs/g CST). The isotherm was fit to the Freundlich/Langmuir Hybrid equilibrium isotherm model (see Hamm et al. 2002) according to Eq. (4.1). The expected Cs loading onto the CST at a given Cs concentration can be determined from the isotherm.

$$\frac{\alpha_i \times [Cs]}{(\beta + [Cs])} = Cs_{IX} \qquad (4.1)$$

where:

[Cs] = equilibrium Cs concentration (mmoles Cs/mL)
Cs_{IX} = equilibrium Cs loading on the CST (mmoles Cs per g CST)
α_i = isotherm parameter constant (mmoles Cs/g CST)[1]
β = isotherm parameter constant (mmoles Cs/mL)[2]

[1] The α_i parameter represents the maximum Cs capacity in the CST (Hamm et al. 2002).
[2] The β parameter incorporates the selectivity coefficients, making it dependent on temperature and composition of all the ionic species in solution; the larger the beta parameter, the less favorable (and lower loadings) an isotherm will be (Hamm et al. 2002).

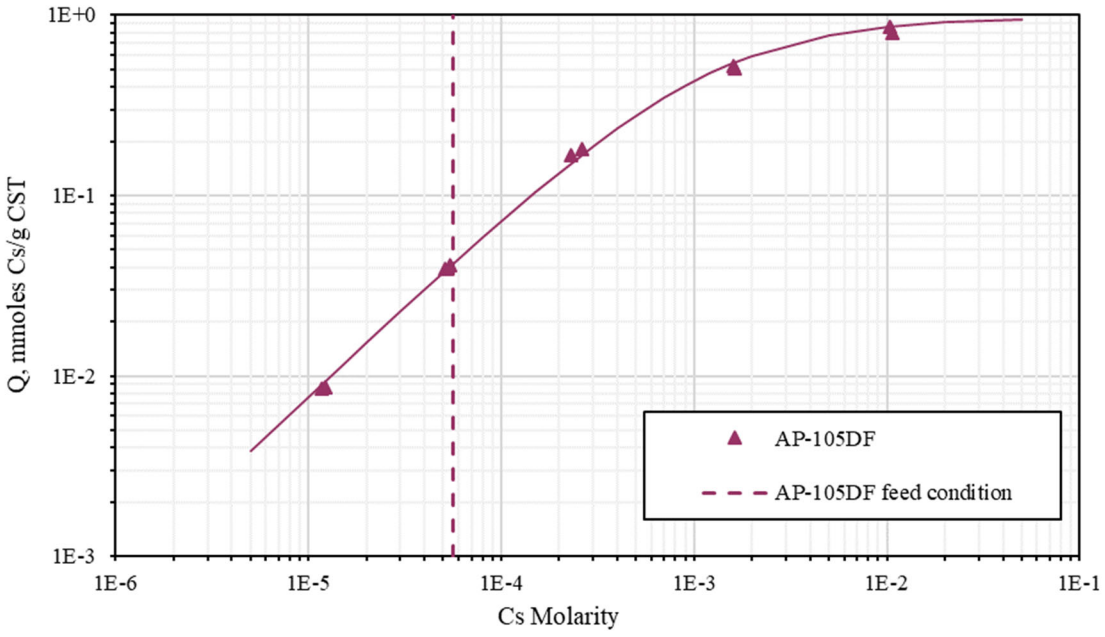

Figure notes: At the equilibrium Cs concentration of 7.58 µg/mL (5.66E-5 M), the equilibrium Cs loading on CST Lot 2002009604 corresponded to 0.0420 mmole Cs per g dry CST (5.63 mg Cs/g CST).

Figure 4.2. Isotherm for AP-105DF Tank Waste with CST Lot 2002009604

The α_i and β parameters for current and past testing are summarized in Table 4.2. As noted previously, both the α_i and the β parameters were significantly higher than those reported by Hamm et al. (2002) (α_i of 0.3944 mmoles Cs/g CST and average β value of 2.8552E-4 M Cs for Envelope A tank waste). The AP-105DF Cs capacity α_i parameter conformed to 0.97 mmoles Cs/g CST, which was higher than previously observed. The AP-105DF β parameter conformed to 1.24E-3 M, which was nearly twice as high as other recent tank waste tests. This indicated that the overall Cs capacity in the AP-105DF matrix was high, but specific matrix effects reduced specificity for Cs exchange at the feed condition.

Table 4.2. α_i and β Parameter Summary

Matrix	CST Lot	α_i, (mmoles Cs/g CST)	β, (Cs M)	Reference
AP-105DF	2002009604	0.97	1.24E-3	This report
1.0 M NaOH/4.6 M $NaNO_3$	2002009604	0.55	5.43E-4	Fiskum et al. 2020
AP-107	2002009604	0.72	7.25E-4	Fiskum et al. 2019b
AW-102	2002009604	0.70	5.84E-4	Rovira et al. 2019
AP-107	2081000057	0.50	5.3E-4[(a)]	Rovira et al. 2018
Envelope A	Not defined	0.3944	2.8552E-4	Hamm et al. 2002

(a) Calculated from reported raw data.

Figure 4.3 compares recent isotherm results with CST Lot 2002009604. The AP-105DF curve fit is offset to the right relative to other curve fits, indicative of lower capacity and concomitant earlier Cs breakthrough in a column run. It is clear, however, that the AP-107 curve fit was not ideal, in that the lowest AP-107 Cs concentration samples appeared to match that of the AP-105DF curve fit. Figure 4.4 examines the same curve in a close-in view around the feed condition. At the AP-105DF feed Cs concentration, the Cs loading for AP-107 is slightly higher than that of AP-105DF and Cs loading from AW-102 is higher than both feeds.

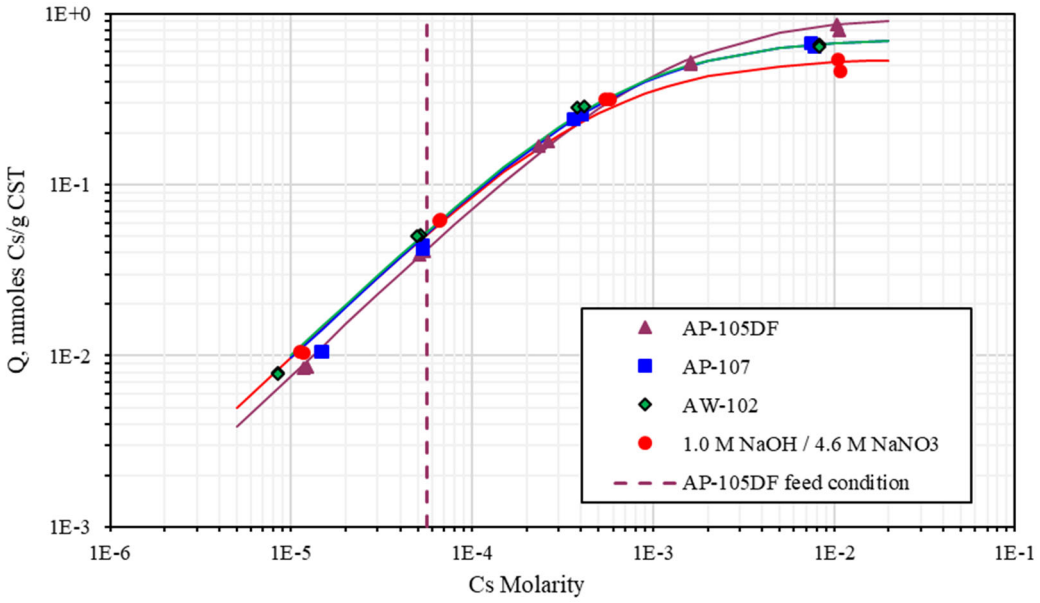

Figure 4.3. Isotherm Comparisons of AP-105DF, AP-107, AW-102, and 1.0 M NaOH/4.6M $NaNO_3$ Simulant with CST Lot 2002009604

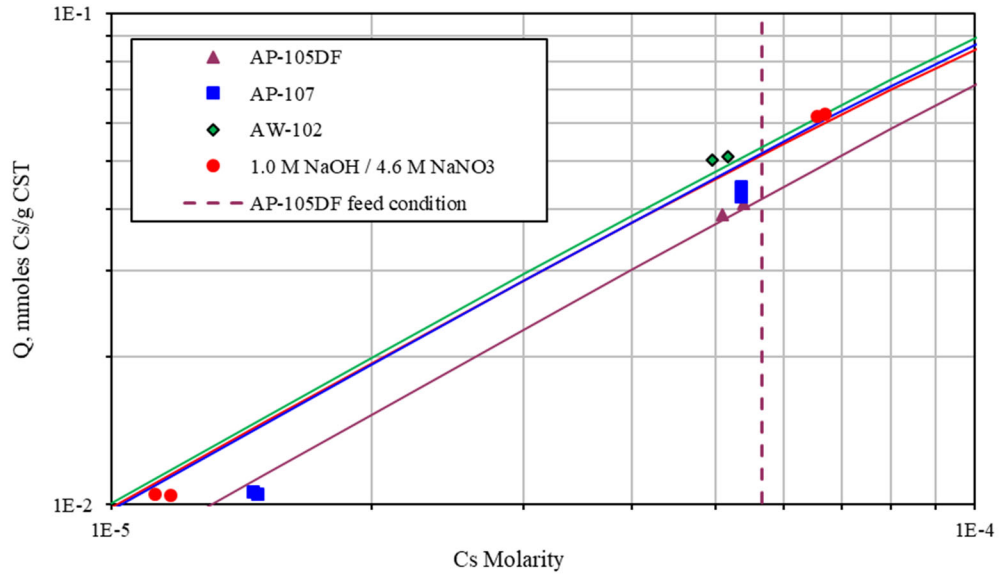

Figure 4.4. Closeup view of the Isotherm Comparisons

Table 4.3 provides the curve-fitted predicted Cs loading at 5.66E-5 M Cs for each feed matrix. The simple simulant result, 1.0 M NaOH / 4.6 M $NaNO_3$, was used as a benchmark (Fiskum et al. 2020). The AP-105DF feed condition Cs loading was ~20% lower than the other matrices. A matrix condition specific to AP-105DF appeared to negatively affect Cs loading relative to other feeds.

Table 4.3. Predicted Cs Loading at 5.66E-5 M Cs Feed Condition with CST Lot 2002009604

Matrix	Predicted Cs Loading (mmole/g CST)	Difference from 1.0 M NaOH / 4.6 M $NaNO_3$ Matrix
1.0 M NaOH/4.6 M $NaNO_3$	0.0516	0%
AP-105DF	0.0420	-19%
AP-107	0.0520[(a)]	+1%[(a)]
AW-102	0.0536	+4%

(a) Likely high bias, see text.

5.0 Column Processing

This section discusses the Cs exchange behavior during the load, FD, water rinse, and final solution flush from the column system. Raw data are provided in Appendix A.

5.1 Cs Loading for AP-105DF, Feed Displacement, and Water Rinse

The AP-105DF feed was processed at nominally 1.83 BV/h through the lead and lag columns for 523 BVs, at which time the lag column effluent reached the WAC limit. The polish column was then placed into position and processing continued. Figure 5.1 shows a linear-linear plot of the cesium load profile for feed processed through each column. The x-axis shows the BVs processed and the y-axis shows the effluent Cs concentration (C) relative to the feed concentration (C_0) in terms of % C/C_0. The C_0 value for ^{137}Cs was determined to be 122 µCi/mL (average of all filtered feeds, relative standard deviation of 1.8%). In this graphing layout, the Cs breakthrough from the lead column appeared to start at ~270 BVs and continued to 92% C/C_0 after processing 1091 BVs when the last sample was collected from the lead column. Similarly, the lag column Cs breakthrough appeared to start at ~650 BVs and increased to 28% breakthrough when the last sample was collected from the column. The polish column Cs breakthrough performance was not discernable at this linear scale.

Figure 5.2 shows the same Cs load data provided in Figure 5.1, but with the ordinate % C/C_0 on a probability scale and the abscissa BVs processed on a log scale. Under normal load processing conditions, these scales provide a straight-line Cs breakthrough curve and provide greater fidelity of load characteristics at low and high % C/C_0 breakthrough values (Buckingham 1967). In contrast to Figure 5.1, the Cs breakthrough from the lead column was observed to start at ~40 BVs processed and breakthrough from the lag column started just after processing 170 BVs. In addition to the 50% C/C_0 indication line, the WAC limit, set at 0.146% C/C_0, is also apparent (dotted red line).[1]

[1] The WAC limit was derived from the allowed curies of ^{137}Cs per mole of Na in the effluent to support contact handling of the final vitrified waste form—3.18E-5 Ci ^{137}Cs/mole Na. At 5.92 M Na and 122 µCi ^{137}Cs/mL in the feed, the WAC limit is 0.155% C/C_0.

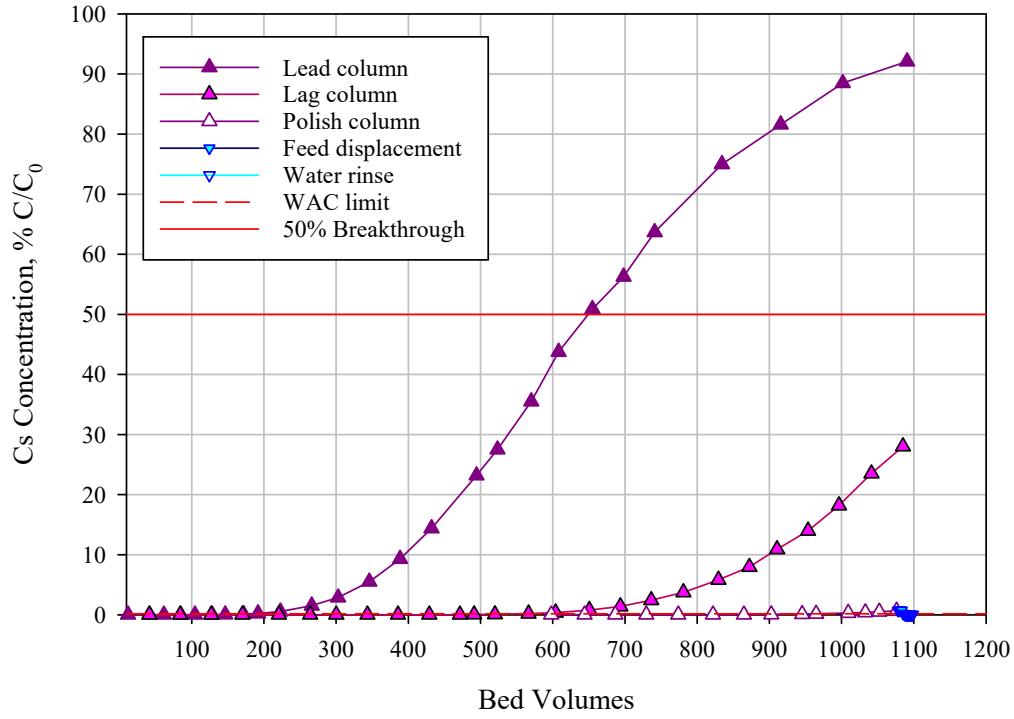

Figure 5.1. Lead, Lag, and Polish Column Cs Load Profiles of AP-105DF at 1.83 BV/h, Linear-Linear Plot

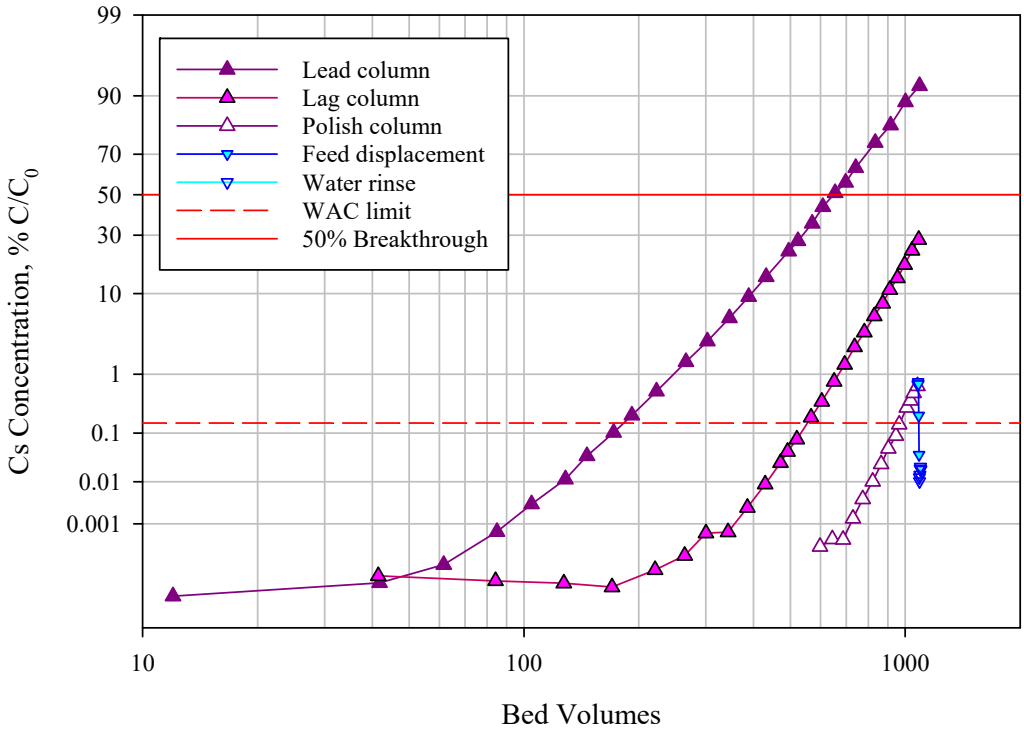

Figure 5.2. Lead, Lag, and Polish Column Cs Load Profiles of AP-105DF at 1.83 BV/h, Probability-Log Plot

The Cs breakthrough curves were modeled by the error function (erf) (Hougen and Marshall 1947; Klinkenberg 1994):

$$\frac{C}{C_0} = \frac{1}{2}\left(1 + \text{erf}\left(\sqrt{k_1 t} - \sqrt{k_2 z}\right)\right) \quad (5.1)$$

where:

k_1 and k_2 = parameters dependent on column conditions and ion exchange media performance
t = time (or BVs processed)
z = column length

Using this model, fits were generated to the lead and lag column experimental data (see Figure 5.3). The lead column breakthrough profile deviated below the model fit starting at ~700 BVs. This indicated non-ideal Cs loading. This is consistent with the differences in capacity seen between the batch contact test and the column test. The batch contact indicates slightly higher capacity than the 50% breakthrough. However, as seen in figure 5.3, the additional cesium is loaded past the 50% breakthrough point (that is, the data fall below the error function fit). These results suggest that the loading kinetics are being retarded in some fashion with this tank waste sample. Potential sources of slower kinetics include the impact of competitor ions (such as calcium) or other constriction to exchange sites. The reader is reminded that significant colloidal solids were found in the solution expelled from the column with compressed air that may be related to occlusion (see Figure 3.7).

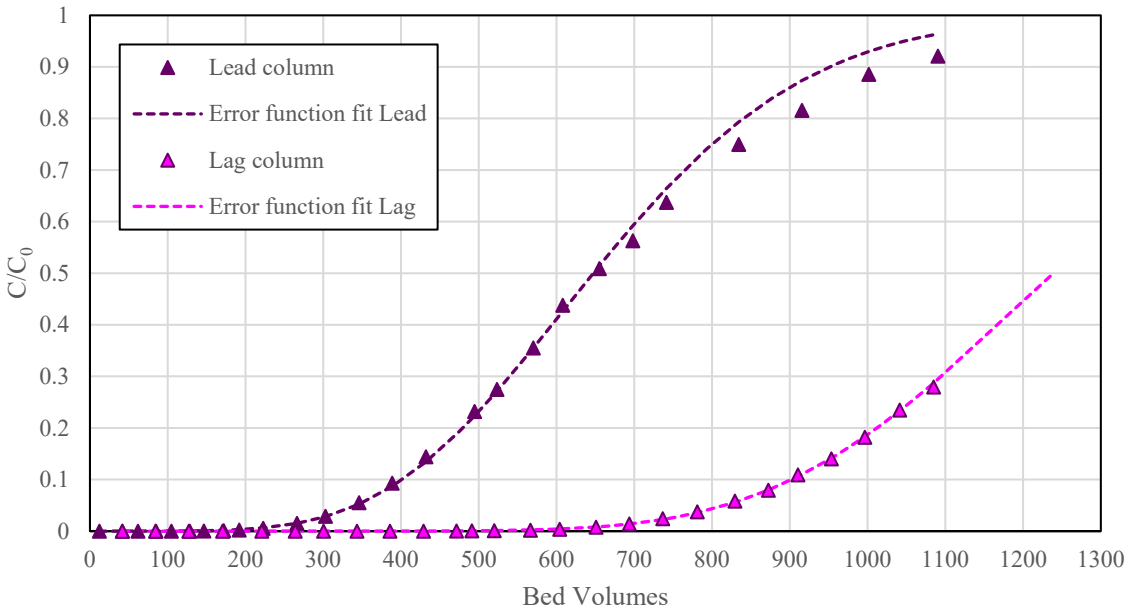

Figure 5.3. Lead and Lag Column Cs Breakthroughs with Error Function Fits

The 50% Cs breakthroughs for the lead and lag columns were estimated from the error function fit at 647 BVs and 1239 BVs, respectively. The lead column 50% Cs breakthrough value was ~15% lower than the 760 BVs Cs λ value predicted from batch-contact studies. The reduced 50% capacity observed during column testing was consistent with the hypothesis that some analyte exchange competition or occlusion was in play during the column run.

The WAC limit Cs breakthroughs were interpolated for each column by curve fitting the BVs processed as a function of the log % C/C_0 values (see Figure 5.4). The curves were fitted to a second-order polynomial function (R^2 = >0.99) and the WAC limits were then easily calculated, resulting in the following:

- Lead column: 187 BVs
- Lag column: 560 BVs
- Polish column: 974 BVs

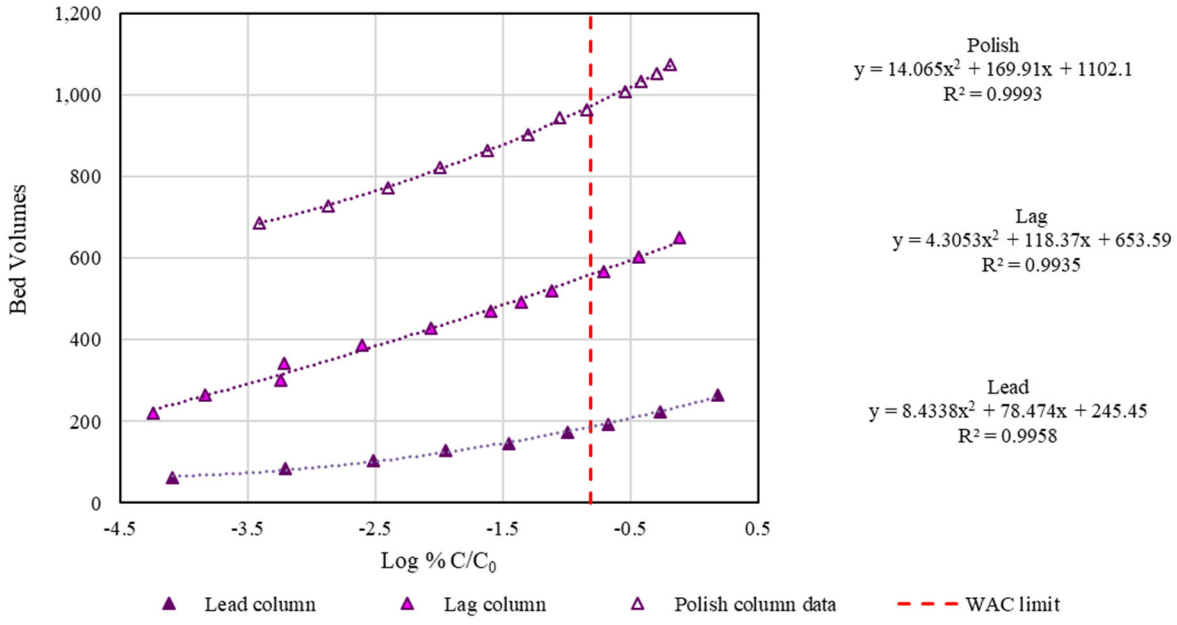

Figure 5.4. Curve Fits to Interpolate WAC Limits from Lead, Lag, and Polish Columns

Figure 5.5 shows the end of the Cs breakthrough profile from the polish column with the FD, water rinse, and the final flushed fluid from the column system on a probability-linear plot. The linear abscissa scale provides better Cs concentration resolution of the various effluent solutions relative to graphing on a log scale. The first 5.4 BVs of the FD simply extended the polish column apparent load curve, consistent with the displacement of residual feed from the system. The Cs concentration began to drop just after processing the seventh BV (one AV), and the effluent Cs concentration continued a downward trajectory. The ensuing water rinse did not result in continued downward Cs concentration; in fact, a slight concentration increase was observed as water rinse progressed. Unlike previous tests with AP-107 and AW-102 where Cs concentrations increased in the water rinse (Fiskum et al. 2019b; Rovira et al. 2019), the Cs concentration in the AP-105DF test water rinse remained relatively static at ~1.6E-2 % C/C_0. As observed previously (Fiskum et al. 2019b; Rovira et al. 2019), the Cs concentration in the solution expelled with compressed air bumped up to the WAC limit. No effort was made to filter this solution prior to ^{137}Cs analysis, so it is not clear if this increased Cs concentration was associated with suspended fines or if a small amount of Cs had exchanged back into solution during the weekend-long contact period with the water rinse.

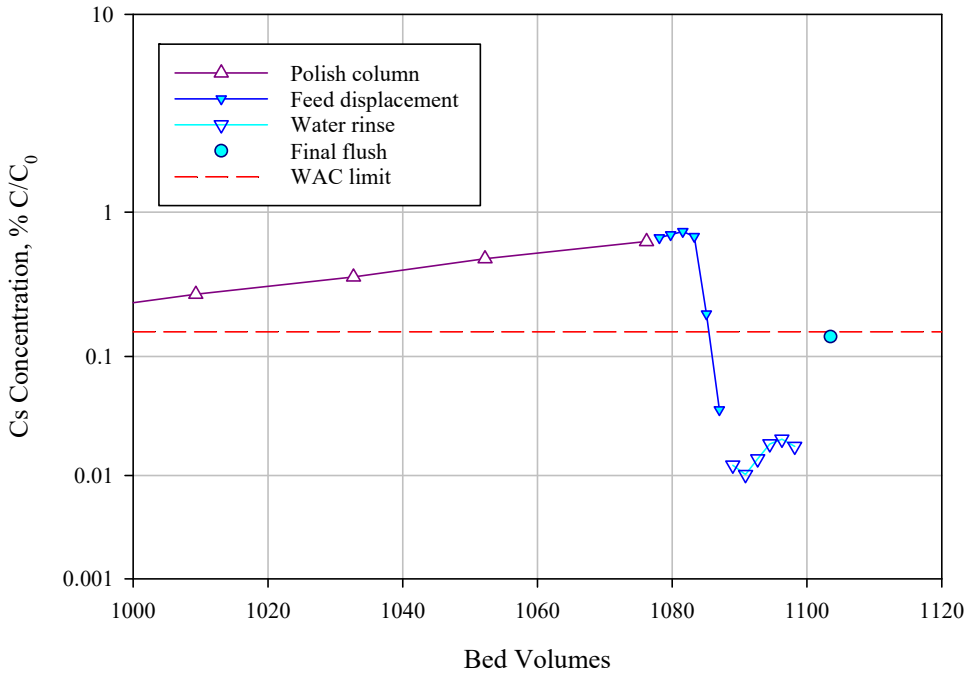

Figure 5.5. AP-105DF Polish Column Cs Load Profile with Feed Displacement, Water Rinse, and Column Flush Solution

Figure 5.6 and Figure 5.7 compare AP-105DF Cs load profiles with AP-107 lead, lag, and polish columns and AW-102 lead and lag columns, respectively. CST Lot 2002009604 was used in all cases; however, the <25-mesh sieve fraction was used for AP-107 and AW102 and the <30-mesh sieve fraction was used for AP-105DF. All else being equal, the smaller sieve fraction would normally result in delayed onset of Cs breakthrough due to higher particle surface area and smaller depth to reach exchange site. The <30-mesh sieve fraction is most prototypic of the full-height column processing (Westesen et al. 2020).

In each case, the AP-105DF Cs breakthrough occurred earlier than those of AP-107 and AW-102, indicative of lower Cs capacity in the AP-105DF matrix at the nominal feed condition. The decreased AP-105DF loading was not kinetically driven, based on the sharper load curve observed with AP-105DF (decreasing kinetic exchange rate corresponds to a lengthening of the load curve). This effect was consistent with the β parameter for AP-105DF being higher than those of AP-107 and AW-102; the β parameter increases with increasing adverse matrix effects on Cs loading (see Section 4.0 of this report and Hamm et al. 2002). It is noted that the K concentration in AW-102 diluted feed was 50% higher (0.153 M) than it was in AP-105DF (0.102 M); K is one of the competitors for Cs on CST. Clearly, K competition was not adversely affecting the difference in Cs load profiles. The hydroxide was ~20% higher in AP105DF relative to AP-107 and AW-102; however, this increase was not expected to impact Cs loading.

There was no clear benefit of positioning the polish column in line after the lag column reached the WAC limit. The Cs breakthrough from the polish column used in AP-107 (present for the entire process) began nearly exactly as the Cs breakthrough from the polish column used in AP-105DF processing (employed when lag column reached the WAC limit). The slight offset observed between these two polish columns was similar to the offset trends established in the lead and lag column performances and therefore is likely not associated with the delayed implementation of the AP-105DF polish column.

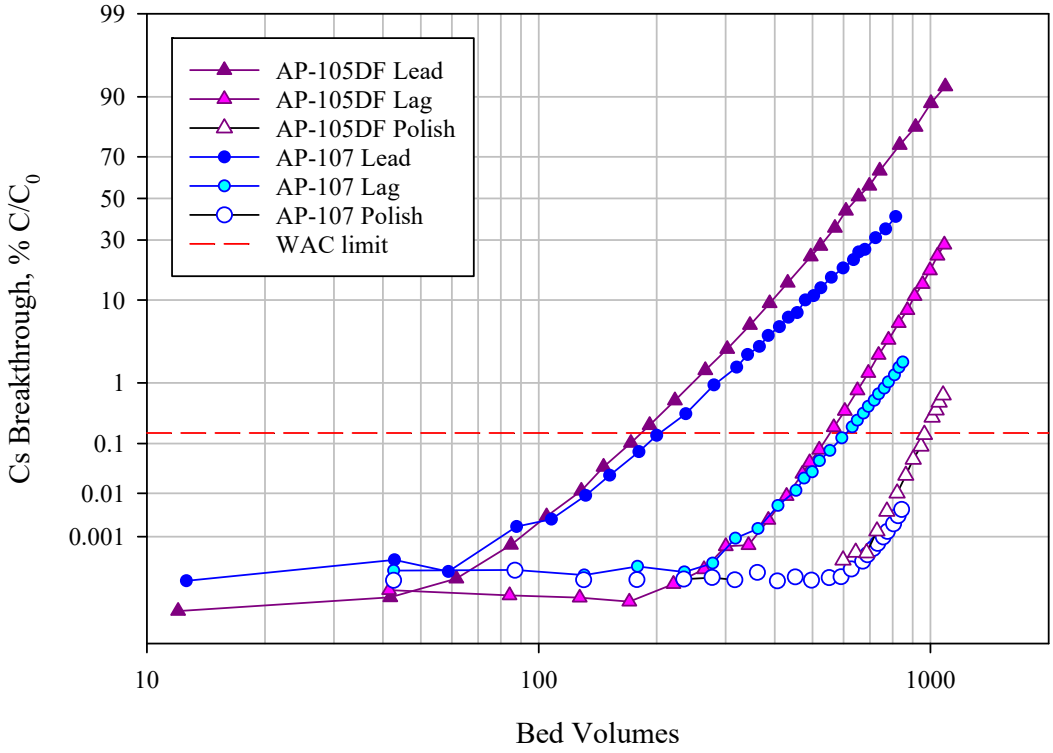

Figure notes:

	AP-105DF	AP-107
Configuration	Lead-lag Lead-lag-polish	Lead-lag-polish
Flowrate, BV/h	1.83	1.88
CST sieve fraction	<30 mesh	<25 mesh
Process Temp. °C	27-29	24-29
Cs, M	5.66E-5	6.91E-5
Na, M	5.92	5.97
K, M	0.102	0.120
OH, M	1.24	0.89
TIC, M	0.472	0.65

Figure 5.6. Load Profile Comparisons: AP-105DF and AP-107 (Fiskum et al. 2019b), CST Lot 2002009604

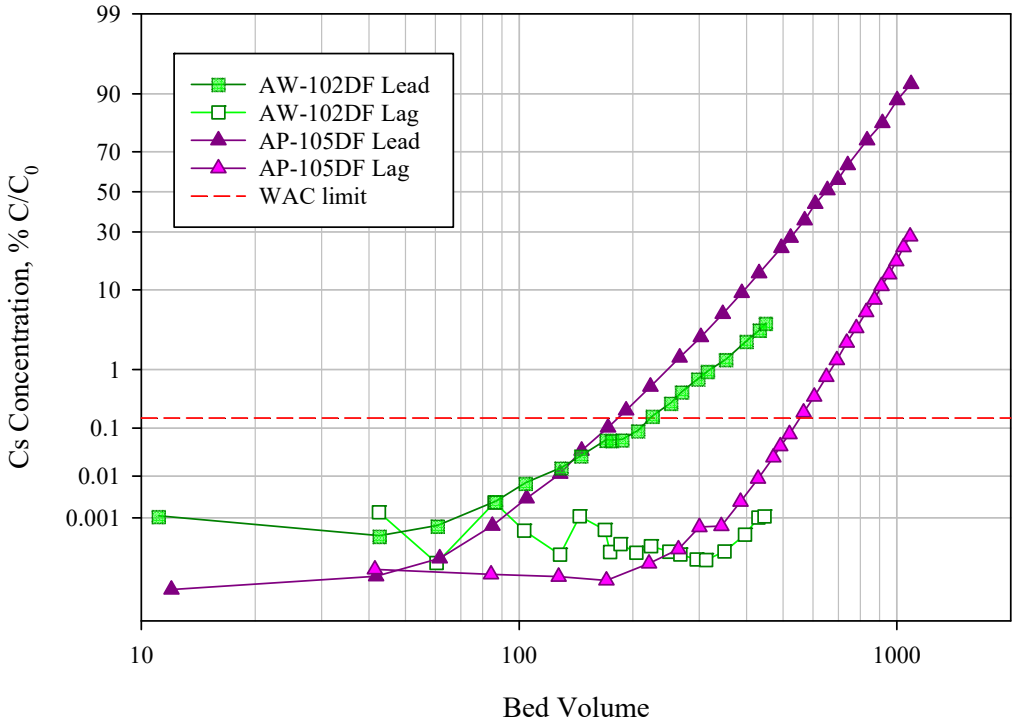

Figure notes:

	AP-105DF	AW-102
Configuration	Lead-lag Lead-lag-polish	Lead-lag
Flowrate, BV/h	1.83	1.81
CST sieve fraction	<30 mesh	<25 mesh
Process Temp. °C	27-29	22
Cs, M	5.66E-5	4.63E-5
Na, M	5.92	5.83
K, M	0.102	0.153
OH, M	1.24	0.98
TIC, M	0.472	0.587

Figure 5.7. Load Profile Comparison: AP-105DF and AW-102 (Rovira et al. 2019), CST Lot 2002009604

5.2 Cesium Activity Balance

The Cs fractionations to the effluents and the columns were determined based on the input ^{137}Cs and the measured ^{137}Cs in the various effluent streams. The quantities of Cs loaded onto the lead, lag, and polish columns were determined by subtracting the Cs recovered in the samples and effluents from the Cs fed to each column. Table 5.1 summarizes the ^{137}Cs fractions found in the various effluents as well as the calculated ^{137}Cs column loadings. About 65% of the total Cs loaded onto the lead column (markedly lower than the 87% found with AP-107 processing, Fiskum et al. 2019b), 31% loaded onto the lag column, and 4% loaded onto the polish column. Sample and effluent collection amounted to ~0.2% of the input Cs.

Table 5.1. ^{137}Cs Activity Balance for AP-105DF

Input	µCi	%
Feed sample	1.33E+06	100
Output		
Effluent-1 (0-128 BVs)	0.029	2.17E-06
Effluent-2 (128-223 BVs)	0.020	1.49E-06
Effluent-3 (223-346 BVs)	0.220	1.65E-05
Effluent-4 (346-474 BVs)	12.3	9.20E-04
Effluent-5 (474-570 BVs)	30.5	2.29E-03
Effluent-6 (570-671 BVs)	0.131	9.86E-06
Effluent-7 (671-792 BVs)	1.82	1.36E-04
Effluent-8 (792-916 BVs)	28.6	2.14E-03
Effluent-9 (916-1023 BVs)	188	1.41E-02
Effluent-10 (1023- 1091 BVs)	364	2.73E-02
Load samples	2119	1.59E-01
Feed displacement, water rinse and flush	78.5	5.89E-03
Total ^{137}Cs recovered in effluents	2,823	2.12E-01
Total ^{137}Cs Column Loading		
Lead column Cs loading	8.66E+05	65.0
Lag column Cs loading	4.11E+05	30.8
Polish column Cs loading	5.37E+04	4.03
Column total	1.33E+06	99.8

The total Cs loaded per g CST was calculated from the total Cs loaded onto the lead column, which was nearly fully saturated under these load conditions (92% Cs breakthrough), and the dry CST mass loaded into the lead column according to Eq. (5.2).

$$\frac{A_{Cs} \times CF}{M} = C \tag{5.2}$$

where

A_{Cs} = activity of ^{137}Cs, µCi on the lead column
CF = conversion factor, mg Cs/µCi ^{137}Cs
M = mass of dry CST (10.0 g)
C = capacity, mg Cs/g CST

A total of 5.39 mg Cs/g CST (0.0402 mmoles Cs/g CST) was loaded onto the lead column. This represented ~95% of the total capacity found from batch contact testing (see Section 4.0). Given that the breakthrough was 92%, the predicted and obtained capacity values agreed well. The total Cs loading capacity in AP-105DF was markedly lower than observed for AP-107 and the 5.6 M Na simulant (see Table 5.2).

Table 5.2. Cs CST Column Loading Comparison

Test	Sieve fraction	CST Cs loading (mg Cs/g CST)	Reference
AP-105DF, 2.4% full height	<30 mesh	5.39	Current report
AP-107, 2.4% full height	<25 mesh	6.76	Fiskum, et al. 2019b
5.6 M Na simulant, 2.5% full height	<25 mesh	6.87	Fiskum et al. 2019c
5.6 M Na simulant, 2.5% full height	<30 mesh	7.63	Rovira et al. 2020
5.6 M Na simulant, 2.5% full height	<35 mesh	7.04	Fiskum et al. 2019c
5.6 M Na simulant, 12% full height	<25 mesh	6.95	Fiskum et al. 2019a
5.6 M Na simulant, 100% full height	As received	6.60	Fiskum et al. 2019a

See Russell et al. (2017) for the 5.6 M Na simulant formulation.

5.3 WAC Limit

Fiskum et al. (2019a,b) demonstrated that the flowrate through the CST column (in terms of BV/h or contact time) directly influences the volume that can be processed before reaching the WAC limit. The authors were able to evaluate the 1-, 2-, and 3-column systems collectively in terms of SV. The AP-105DF data collected from the lead and lag columns were also evaluated in this manner. The AP-105DF polish column only incorporated the volume associated with its usage interval from 523 BV to 1091 BV and therefore was not fully comparable to a 3-column system where the third column was in position for the test duration.

The SV/h in the lead column was, by definition, equivalent to the BV/h flowrate. The combined lead-lag column, with two sequential 10-mL CST beds, corresponded to half this flowrate. The 3-column system, with three sequential 10-mL CST beds, corresponded to a third of this flowrate. The AP-015DF SVs, adjusted flowrate, and SVs to WAC limit are provided in Table 5.3. These data are also superimposed on the previously reported graphed data set in Figure 5.8. The AP-105DF data points lie under the curve established for the 5.6 M Na simulant (simulant formulation reported by Russell et al. 2017). Like AP-107, fewer AP-105DF BVs can be processed to reach the WAC limit than predicted by the simulant, indicative that components in the tank wastes were consuming or otherwise affecting exchange sites that were not well modeled by the simulant.

Table 5.3. Bed Volumes Processed to Reach WAC Limit

AP-105DF Systems	SV (mL)	Flowrate (SV/h)	SVs to WAC Limit
Lead column	10	1.83	187
Lead-lag column	20	0.92	280
Lead-lag-polish column	30	0.61	325[(a)]

(a) The polish column was only in position during second half of processing interval from 523 BV to 1091 BV and may not be truly representative of the 30-mL CST bed (3-column system) configuration.

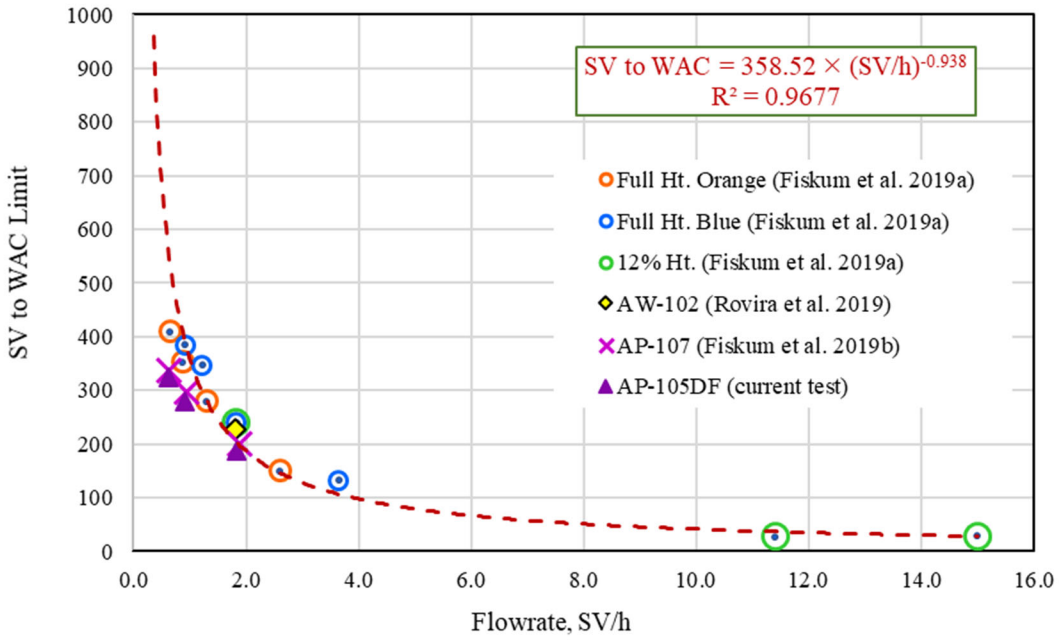

Figure 5.8. System Volume to WAC Limit vs. Flowrate with CST Lot 2002009604

Figure notes:

- Fiskum et al. 2019a, 5.6 M Na simulant test matrix.
  - Orange and Blue column data collected from four serial ~0.592-L CST beds, unsieved CST, 2.54-cm-diameter column.
  - Medium column data were collected from single 44-mL CST beds, <25-mesh CST, 1.5-cm-diameter column.
- AW-102 datum collected from single 10-mL CST bed (lead column), <25-mesh CST, 1.5-cm inside diameter. The WAC limit was re-evaluated to be 226 BVs.
- AP-107 column data were collected from three serial 10-mL CST beds; the left-most data point from the polish column was extrapolated, <25-mesh CST, 1.5-cm-diameter column

5.4 Transition Zone

The transition (or exchange) zone is defined as the volume processed from the onset of Cs breakthrough to the full saturation of the ion exchanger where the effluent Cs concentration equals the influent Cs concentration and the 50% Cs breakthrough point is the inflection point around which the transition zone pivots. In the current study, the lead column was loaded to 92% Cs breakthrough; the 50% breakthrough was interpolated at 647 BVs. The number of BVs processed between 20% and 50% Cs breakthrough was calculated from the load curve. This value was doubled to determine the 20% to 80% Cs breakthrough transition zone: 341 BVs. Similarly, the transition zone between 5% and 95% Cs breakthrough was calculated: 626 BVs. Table 5.4 compares the transition zones determined for AP-105DF, AP-107, and 5.6 M Na simulant. The AP-105DF transition zone was hundreds of BVs shorter than those determined with AP-107 and 5.6 M Na simulant. The fundamental reason for a decreased transition zone is not understood at this time.

Table 5.4. Transition Zone Comparison, CST Lot 2002009604

Test	Flowrate (BV/h)	BVs to Cs Breakthrough			Transition Zone (BVs)	
		(5%)	(20%)	(50%)	(20-80%)	(5-95%)
AP-105DF	1.83	334	477	647	341	626
AP-107 (Fiskum et al. 2019b)	1.88	400	620	~900	~560	~1000
Blue (Fiskum et al. 2019a)[(a)]	1.82	492	700	~1050	~700	~1120

(a) 5.6 M Na simulant matrix

5.5 Chemical and Radiochemical Composition

The AP-105DF composite feed and composite effluent samples underwent extensive characterization to better define waste characteristics and assess analyte fractionation to the CST. Ten lead column samples were also selected for metal and radionuclide analysis to assess analyte load characteristics (41.8, 84.9, 128, 172, 223, 303, 389, 495, 741, and 1091 BVs).

Table 5.6 summarizes the feed and effluent metals concentrations and fractionations to the effluent. The anions, free hydroxide, inorganic carbon, and organic carbon concentrations in the effluent are provided in Table 5.7; they were not measured in the feed because it was shown that their concentrations were not affected by the CST processing (Rovira et al. 2018). Further, bench handling of the effluent was safer for the analysts from a radiological dose perspective. Analytical reports along with result uncertainties and quality control discussions are provided in Appendix C.

By inference, the analytes present in the feed and not found in the effluent were assumed to be retained on the CST. Analyte fractionation was calculated as the ratio of the total analyte measured in the feed processed through the columns and the total analyte collected in the Cs-decontaminated effluent according to Eq. (5.3):

$$\frac{C_{Da} \times V_D}{C_{Fa} \times V_F} = F_{Da} \tag{5.3}$$

where:

C_{Da} = concentration of analyte *a* in the Cs-decontaminated effluent
V_D = volume of Cs-decontaminated effluent
C_{Fa} = concentration of analyte *a* in the AP-105DF feed
V_F = volume of AP-105DF feed
F_{Da} = fraction of analyte *a* in the Cs-decontaminated effluent

The analyte results shown in brackets indicate the result was less than the instrument EQL but greater than or equal to the MDL; the associated analytical uncertainty could be higher than ±15%. The fractionation result was placed in brackets, where it was calculated with one or more bracketed analytical values to highlight the higher uncertainty. The opportunistic analyte results measured by ICP-OES are also shown in Table 5.6; these analytes are part of the ICP-OES data output but have not been fully evaluated for quality control performance.

Table 5.5. AP-105DF Feed and Effluent Radionuclide Concentrations and Fractionations (ASR 1097)

Analysis Method	Analyte	TI082-Comp-Feed (µCi/mL)	TI082-Comp-Eff (µCi/mL)	Fraction in Effluent (%)
Gamma energy analysis (GEA)[a]	^{60}Co	<5.8E-04	4.05E-04	--
	^{137}Cs	1.13E+02[b]	5.36E-02	0.047
	^{154}Eu	<2.7E-03	7.52E-05	--
Separations/ Alpha energy analysis (AEA)[a]	^{237}Np	6.69E-06	1.22E-06	18
	^{238}Pu	6.37E-06	2.64E-06	41
	$^{239+240}$Pu	3.94E-05	1.56E-05	39
	^{241}Am	2.66E-04	2.30E-04	86
Separations/ Beta counting[a]	^{90}Sr	6.90E-01	7.23E-04	0.10
	^{99}Tc	1.13E-01	1.05E-01	93

(a) Reference date is December 2020.
(b) ^{137}Cs measured in the individual feed samples was 122 µCi/mL (see Section 3.2); the 113 µCi/mL value was 8% lower and was not considered statistically different given the overall experimental uncertainty and decay correction.
"--" = not applicable; value not reported, or fractionation cannot be calculated with a less-than value.
The recovered fractions are calculated with values containing more significant figures than shown; using listed values may result in a slight difference due to rounding.

Table 5.6. AP-105DF Feed and Effluent Inorganic Analyte Concentrations and Fractionation (ASR 1097)

Analysis Method	Analyte	TI082-Comp-Feed (M)	TI082-Comp-Eff (M)	Percent in Effluent
ICP-OES	Al	5.26E-01	5.23E-01	99%
	As	<5.5E-04	[9.7E-04]	--
	Ca	1.03E-03	1.02E-03	99%
	Cd	[2.4E-05]	[2.0E-05]	--
	Cr	6.43E-03	6.56E-03	101%
	Fe	[2.0E-05]	<1.6E-05	--
	K	1.02E-01	1.02E-01	100%
	Na	5.92E+00	6.00E+00	101%
	P	1.27E-02	1.44E-02	113%
	S	4.66E-02	4.65E-02	99%
	Ti	<5.9E-06	[2.3E-05]	NA
	Zn	[4.6E-05]	[4.7E-05]	--
	Zr	<9.4E-06	[4.5E-05]	NA
ICP-MS	Ba	<1.6E-06	<1.3E-06	--
	Nb	2.74E-07	2.89E-05	NA
	Pb	9.00E-05	2.67E-05	29%
	Sr	1.82E-06	1.64E-07	8.9%
	^{238}U	2.46E-05	1.99E-05	80%

Table 5.6 (cont.)

Analysis Method	Analyte	TI082-Comp-Feed (M)	TI082-Comp-Eff (M)	Fraction in Effluent
ICP-OES Opportunistic Analytes	Ag	<1.2E-05	<1.0E-05	--
	B	5.00E-03	4.56E-03	91%
	Ba	[4.9E-06]	[1.3E-06]	--
	Be	[1.9E-05]	[1.7E-05]	--
	Bi	[1.1E-04]	[7.7E-05]	--
	Ce	[4.9E-05]	[3.8E-05]	--
	Co	<4.1E-05	<3.4E-05	--
	Cu	[4.0E-05]	[2.6E-05]	--
	Dy	<8.8E-06	<7.3E-06	--
	Eu	<3.2E-06	<2.7E-06	--
	La	<8.2E-06	<6.8E-06	--
	Li	<1.3E-04	<1.0E-04	--
	Mg	<4.3E-05	<3.6E-05	--
	Mn	<2.5E-06	<2.0E-06	--
	Mo	4.89E-04	4.98E-04	101%
	Nd	<5.0E-05	<4.1E-05	--
	Ni	4.86E-04	5.35E-04	110%
	Pb	<7.8E-05	<6.5E-05	--
	Pd	<3.0E-05	<2.5E-05	--
	Rh	<8.8E-05	<7.3E-05	--
	Ru	[8.6E-05]	[7.8E-05]	--
	Sb	<3.5E-04	<2.9E-04	--
	Se	[9.1E-04]	<6.5E-04	--
	Si	3.72E-03	3.06E-03	82%
	Sn	<1.4E-04	<1.2E-04	--
	Sr	<1.4E-06	<1.2E-06	--
	Ta	<1.2E-04	<9.6E-05	--
	Te	<9.0E-05	<7.4E-05	--
	Th	<2.1E-05	<1.7E-05	--
	Tl	[3.3E-04]	<7.4E-05	--
	U	[1.4E-04]	<8.3E-05	--
	V	<1.5E-05	<1.2E-05	--
	W	4.26E-04	4.07E-04	95%
	Y	<4.6E-06	<3.8E-06	--

Bracketed values indicate the associated sample results were less than the EQL but greater than or equal to the MDL. Analytical uncertainty for these analytes was > ±15%.

"--" indicates the recovery could not be calculated.

NA = not applicable; Nb, Ti, and Zr are components of CST

The recovered fractions are calculated with values containing more significant figures than shown; using listed values may result in a slight difference due to rounding.

Table 5.7. AP-105DF Effluent Anions and Carbon Composition (ASR 1097)

Analysis Method	Analyte	TI082-Comp-Feed (M)
Titration	Free Hydroxide	1.24
Ion Chromatography	F^-	<2.6E-04
	Cl^-	1.10E-01
	NO_2^-	1.38E+00
	NO_3^-	1.89E+00
	PO_4^{3-}	8.72E-03
	$C_2O_4^{2-}$	2.84E-03
	SO_4^{2-}	2.44E-02
Hot persulfate oxidation	Total organic C	2.16E-01
	Total inorganic C[(a)]	4.72E-01

(a) Assumed to be carbonate.

In addition to Cs removal, the CST removed 99.9% of the ^{90}Sr with a ^{90}Sr decontamination factor of 959. The reduced Sr decontamination (91.1%) measured by ICP-MS may have been confounded with Sr isobaric interferences. The radiochemical analysis was considered more reliable with specificity for ^{90}Sr and stable Sr and ^{90}Sr were expected to behave similarly. About 82% of the Np and 60% of the Pu were also removed. The Np and Pu removal factors were consistent with those previously reported (Rovira et al. 2018, Fiskum et al. 2019b). About 14% of Am was calculated to be removed during processing; the chemistry involved in Am removal by CST is not known. Assuming the difference in total Am, Np, and Pu µCi content between the feed and effluent remained with the lead column CST (10 g), the CST would contain 77 nCi/g transuranic (TRU) isotopes, which is under the threshold 100 nCi/g defining TRU waste. Most of ^{99}Tc, 93% (likely present as anionic pertechnetate), was found in the effluent showing minimal Tc interaction with the CST.

The ICP-OES results for the feed composite and effluent composite showed that the majority of analytes remained in the effluent (see Table 5.6 and Appendix C for analytical reports). The Al, Ca, Cr, K, Na, P (phosphate), and S (sulfate) partitioned exclusively to the effluent (>99% recovery). The effluent recoveries of Ca, Pb, and U were higher than expected in the AP-105DF test because previous tests showed much lower analyte recoveries (see analyte recovery summary in Table 5.8). Three possible drivers likely led to the higher analyte recoveries.

1. The AP-105DF process volume was larger than those of previous tests; thus, more analyte would break through into the effluent based on a short breakthrough curve.
2. The analyte concentrations were slightly higher in AP-105DF, and exchange sites may have been consumed more quickly. Table 5.9 compares the feed analyte concentrations.
3. The soluble analytes were complexed differently in AP-105DF, leading to less CST uptake.

Table 5.8. Ca, Pb, Sr, U Effluent Recovery Comparisons

Tank	BVs	Ca	Pb	Sr	U
AW-102[(a)]	450	[38%]	NA	0.20% (^{90}Sr)	68%
AP-107[(b)]	855	[52%]	NA	<0.2% (^{90}Sr)	61%
AP-105DF	1091	99%	29%	8.9%	80%

(a) Rovira et al. 2019
(b) Fiskum et al. 2019b
NA = not applicable, the analyte was not detected in the effluent.

Table 5.9. Ba, Ca, Pb, Sr, U Feed Concentration Comparisons

Tank	Ba, M	Ca, M	Pb, M	Sr, M	U, M
AW-102[(a)]	[3.7E-6]	[6.0E-4]	<3.9E-5	<2.9E-6	7.48E-4
AP-107[(b)]	[3.0E-6]	[8.6E-4]	[3.9E-5]	[1.5E-6]	7.51E-5
AP-105DF	<1.6E-6	1.03E-3	9.00E-5	1.82E-6	2.46E-5

(a) Rovira et al. 2019
(b) Fiskum et al. 2019b

The Ba, Ca, Sr, and U analyte concentrations differed slightly between the three tank wastes, with just slight elevations in the Ca and Pb concentrations in AP-105DF relative to those measured in AW-102 and AP-107. However, Ca and Pb were not found to have much effect on CST Cs uptake (Fiskum et al. 2020). It is unlikely that these slight elevated concentrations would result in an earlier Cs breakthrough profile with a shorter transition zone.

The load behaviors of selected analytes were examined as a function of BVs processed through the lead column. (Raw data are provided in Appendix B.) Figure 5.9 shows the Al, Ca, Pb, Sr, and U breakthrough results along with the Cs breakthrough profile. The Al breakthrough serves as an "internal standard" for comparison of the ICP-OES analysis results; its breakthrough remained at 99% ±3% throughout the analytical run.

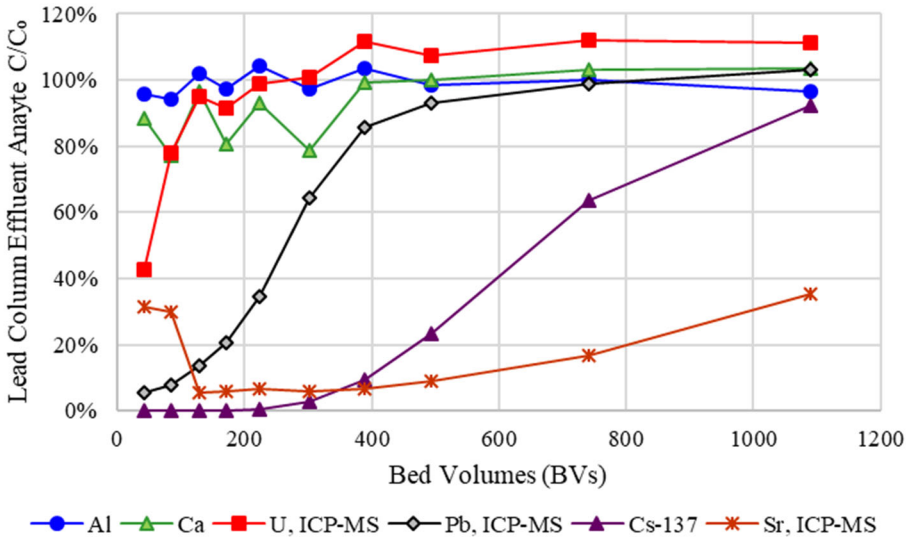

Figure 5.9. Al, Ca, Cs, Pb, Sr, and U Load Profiles from the Lead Column

The Ca results showed somewhat erratic breakthrough behavior (77% to 96% breakthrough) through ~400 BVs processed, at which point it leveled out to 100% breakthrough. The immediate and high Ca breakthrough indicated minimal interaction of Ca occurred on the CST bed. This behavior contrasted with AW-102 and AP-107, where ~40 to 60% Ca breakthroughs were observed (Rovira et al. 2019 and Fiskum et al. 2019b, respectively). Ca may have complexed differently in the AP-105DF by hydroxide, carbonate, and/or organic chelators mitigating CST interaction.

The U broke through rapidly reaching steady state after processing ~390 BVs. The consistent overshoot of 100% breakthrough (390 to 1091 BVs) suggested that the feed U analysis result may have been biased ~10% low or the individual (2-mL) samples may have concentrated slightly from evaporation. The U

50% breakthrough occurred at ~50 BVs, indicating a short transition zone and minimal uptake by CST. These results were generally consistent with Oak Ridge National Laboratory (ORNL) W-27 tank waste (Walker Jr. et al. 1998), where U 50% breakthrough occurred at ~90 BVs, and AP-107 tank waste (Fiskum et al. 2019b), where 50% U breakthrough occurred at ~100 BVs.

The Pb breakthrough occurred intermediate to U and Cs breakthroughs reaching 50% breakthrough after processing ~260 BVs. Comparisons to previous testing of AP-107 and AW-102 tank wastes with this CST lot were not possible because Pb was not measured above the MDL in the column effluent samples. Walker Jr. et al. (1998, Figure 26) reported a Pb breakthrough curve with ORNL W-27 tank waste; in that case 50% Pb breakthrough occurred later at ~400 BVs.

Sr breakthrough measured by ICP-MS was evident, reaching 35% breakthrough after processing 1091 BVs. Sr breakthrough was not detectable in AP-107 or AW-102 processing.

Similarly, the selected lead column effluent samples were analyzed for ^{90}Sr, ^{237}Np, ^{238}Pu and $^{239+240}$Pu. Figure 5.10 shows the load profiles for ^{90}Sr, ^{237}Np, and $^{239+240}$Pu isotopes in comparison with that of ^{137}Cs. The ^{90}Sr breakthrough profile did not show the leading high Sr values at 42 and 85 BVs (as measured by ICP-MS) and it converged with that measured by ICP-MS at ~494 BVs. ^{90}Sr breakthrough was measurable from the first collected sample (see Appendix B). This Sr load behavior was unlike that found in testing with AP-107 where ^{90}Sr concentrations hovered near the detection limit (1.0E-3 µCi/mL) through 558 BVs processed (Fiskum et al. 2019b). The Np breakthrough profile showed increasing effluent concentration from 15% to 77% in the 42 to 1091 BVs range; AP-107 processing resulted in steady-state Np 60% breakthrough once 280 BVs were processed (Fiskum et al. 2019b). The ^{238}Pu results were reported with higher uncertainty and the associated C/C_0 values were more erratic than those of $^{239+240}$Pu. Therefore, the ^{238}Pu values were not further evaluated. The Pu demonstrated an initial 40% breakthrough and very slowly increased to 60% breakthrough to the end of testing. The Pu breakthrough profile was generally consistent with that measured from AP-107 processing (Fiskum et al. 2019b).

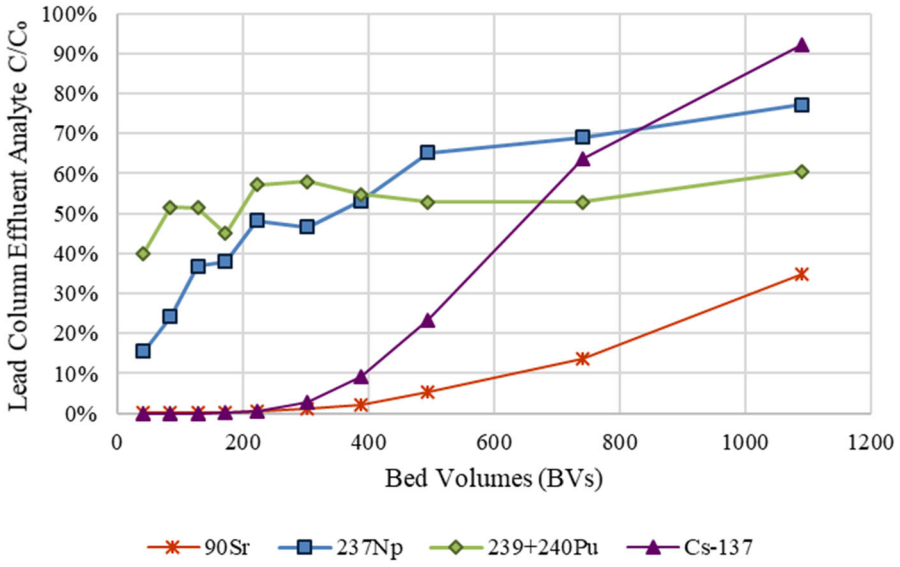

Figure 5.10. ^{90}Sr, ^{137}Cs, ^{237}Np, and $^{239+240}$Pu Load Profiles onto the Lead Column

Figure 5.11 shows the small concentrations of Nb, Ti, and Zr observed in each of the selected lead column effluent samples (see Appendix B for feed and effluent sample concentrations). Neither Ti nor Zr were detected in the feed; only a small amount of Nb was detected in the feed relative to the effluent (2.7E-7 M Nb). Therefore, it was inferred that some small loss of CST components occurred during processing. It is not clear if this loss is due to attrition from extraneous material associated with production or an actual loss of the CST bed. The total Nb, Ti, and Zr masses recovered in the 10.9 L AP-105DF effluent were small and likely would not generate issues with downstream vitrification activities: 0.029 g Nb, ~0.012 g Ti, and ~0.045 g Zr.

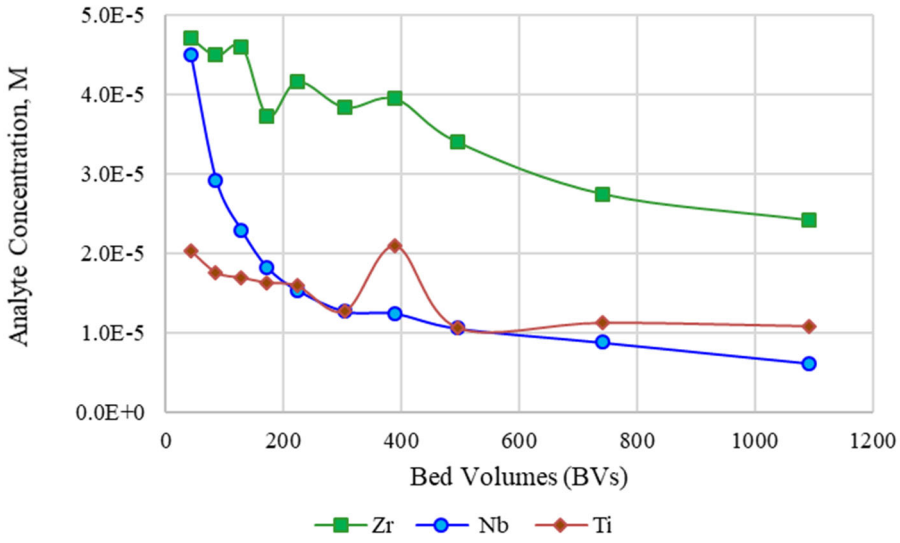

Figure 5.11. Nb, Ti, and Zr Effluent Profiles from the Lead Column

Figure note: The feed analyte concentrations were 2.74E-7 M Nb, <5.9E-6 M Ti, and <9.4E-6 M Zr

5.6 Colloidal Solids Recovered in Flushed Solution

Solids were observed in the final fluid flushed from the column with compressed air. Solids in the flush solution have not been previously observed. The solids were brownish gray and colloidal in nature (see Section 3.4.2). After a settling period, the bulk of the fluid was removed, and the solid residue was evaporated to dryness in the hot cell at cell temperature. The solids were acid digested and analyzed by ICP-OES (per ASR 1109). Table 5.10 provides the result of the targeted analytes along with the opportunistically measured analytes. Collectively, the measured solids represented 35 wt% of the submitted sample; the balance of mass is likely associated with anions (hydroxide, nitrate, nitrite, etc.) and oxides. Figure 5.12 compares the collected solids and AP-105DF tank waste analyte concentrations normalized to Na (molar basis).

Table 5.10. Flushed Solids ICP-OES Analysis (ASR 1109)

Targeted		Opportunistic			
Analyte	TI082-Flush Solids (µg/g)	Analyte	TI082-Flush Solids (µg/g)	Analyte	TI082-Flush Solids (µg/g)
Al	42,200	Ag	[5.3]	Mo	[6.9]
Ca	4,865	As	[123]	Nd	512
Cr	61,800	B	291	Pd	87.4
Fe	8,075	Ba	555	Rh	<15
K	1,890	Be	7.99	Ru	[10]
Na	136,500	Bi	[61]	Sb	[245]
Ni	29,150	Cd	692	Se	<102
P	[220]	Ce	86.3	Sn	[28]
Pb	3,545	Co	[23]	Sr	22.6
S	[500]	Cu	1,090	Ta	<34
Si	5,595	Dy	<2.3	Te	[74]
Ti	5,220	Eu	[5.8]	Th	185
Zn	961	La	116	Tl	<30
Zr	1,910	Li	78.5	U	[69]
		Mg	43,300	W	[9.4]
		Mn	401	Y	<13

Bracketed results were less than the estimated quantitation limit but greater than or equal to the method detection limit.
Opportunistically measured analytes are part of the ICP-OES data output but have not been fully evaluated for quality control performance.

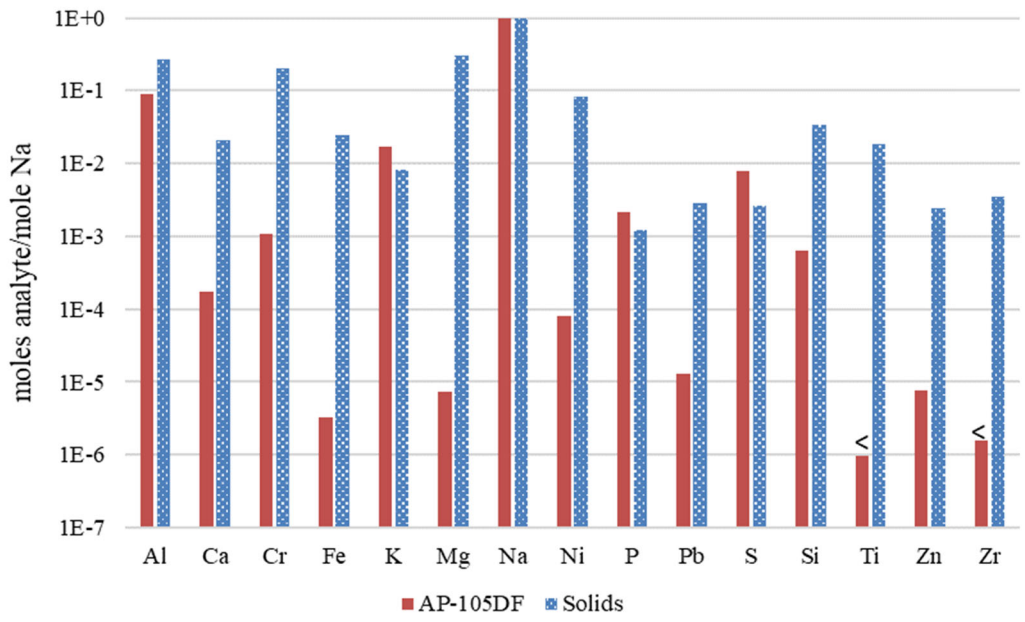

Figure 5.12. Comparison of Solids Flushed from CST Columns and AP-105DF Normalized to Na

Figure Note: Ti and Zr were less-than (<) values in the feed.

The Na is presumed to be largely associated with carryover from residual tank waste and 0.1 M NaOH flush solution. The solids S/Na, P/Na, Al/Na, and K/Na mole ratios are similar to those of the feed and are

thus likely associated primarily with the residual salts from tank waste. The Ca/Na and Si/Na are higher in the solids; in combination with the slightly higher mole ratio observed for Al/Na in the solids, these may be associated with cancrinite. Of the remaining metals, the mole ratio differences between the solids and the AP-105DF decrease in the following order: Mg/Na > Cr/Na > Ni/Na > Fe/Na > Pb/Na >Zn/Na. It is not clear where the relatively large fractions of Mg, Cr, Ni, Fe, Pb, and Zn arise. Ba and Sr were detected in the solids (see Table 5.10). Ba, Pb, and Sr exchange onto CST and may be associated with CST fines blown from the columns. Ti and Zr were also present in the solids, again indicative of some amount of CST fines in these solids (Nb was not measured).

6.0 Conclusions

Cesium ion exchange batch contact testing and column testing were conducted with CST Lot 2002009604 sieved to <30 mesh to assess Cs exchange performance with AP-105DF tank waste. Column testing was conducted at a small scale in the RPL hot cells to accommodate the high radiological dose rate of the Hanford tank waste matrix. The results summary is provided below.

6.1 Batch Contact Testing

Batch contact testing with five Cs concentrations in the AP-105DF matrix was conducted to develop Cs K_d and isotherm curves. Duplicate tests were conducted, each mixed for 72 h at nominally 30 °C cell temperature. The following conclusions were made as a result of this work.

1. The calculated ^{137}Cs K_d value of 760 mL AP-105DF/g CST at Cs equilibrium condition of 7.58 µg Cs/mL (5.66E-5 M Cs) corresponded to a predicted 50% Cs breakthrough of 760 BVs. The measured 50% Cs breakthrough in the column testing was 15% lower (647 BVs) than predicted, indicating that a competitor or other matrix condition was challenging Cs exchange in the dynamic column system.

2. The Cs load capacity at 7.58 µg Cs/mL (5.66E-5 M Cs) equilibrium condition was 0.0420 mmoles Cs/g CST (5.63 mg Cs/g CST). Column testing resulted in lower achieved Cs loading on the lead column, 0.0402 mmoles Cs/g CST or 95% of the predicted capacity measured by batch contacts (the lead column Cs breakthrough reached 92%).

3. The maximum Cs load capacity was measured at 0.966 mmoles Cs/g CST based on a Freundlich/Langmuir hybrid equilibrium fit. This was a higher total capacity than previously measured with AW-102 (0.719 mmoles Cs/g CST) and AP-107 (0.718 mmole Cs/g CST).

4. The Cs capacity in the AP-105DF matrix was about 20% less than found with AP-107, AW-102, and 1.0 M NaOH/4.6M $NaNO_3$ simulant at the AP-105DF feed Cs concentration (5.66E-5 M Cs) even though the total Cs capacity was higher in the AP-105DF matrix.

6.2 Column Testing

AP-105DF tank waste was processed through two columns sequentially positioned in a lead-lag format; after processing 523 BVs, a polish column was placed in line. Each column was filled with 10.0 mL of CST ion exchanger. A total of 10.9 L of AP-105DF tank waste, containing 5.92 M Na and 122 µCi/mL ^{137}Cs, was processed through the Cs ion exchange system at 1.83 BV/h. Effluent samples were collected periodically from each column during the load process and measured for ^{137}Cs to establish the Cs load curves. The flowrate was increase to 2.9 BV/h to process 11 BVs each of 0.1 M NaOH FD and water rinse. The following conclusions were made as a result of the column test.

1. A total of 647 BVs of AP-105DF tank waste, processed at 1.83 BV/h, can be treated before reaching 50% Cs breakthrough on the lead column.

2. The lag column reached the WAC limit when 560 BVs of AP-105DF feed was processed. The effluent from the polishing column reached the WAC limit after processing 974 BVs.

3. FD resulted in decreasing Cs concentration coming off the polish column once the SV was removed, but the subsequent water rinse resulted in slightly increased effluent Cs concentration that remained well below the WAC limit.

4. The AP-105DF Cs breakthrough profile was compared with those of AP-107 (Fiskum et al. 2019b) and AW-102 (Rovira et al. 2019). Although onsets of Cs breakthroughs were similar, the AP-105DF Cs breakthrough was steeper from all three columns relative to those found with AP-107. Similar observations were found relative to AW-102. The steeper AP-105DF Cs breakthrough load curve (shorter transition zone) indicated that a matrix effect was challenging the Cs loading.

5. There was no substantive improvement in the Cs breakthrough from the polish column with its late placement in line to the exchange system relative to results from AP-107 processing. The BVs processed to reach the WAC limit from the polish column with AP-105DF was interpolated to 974 BVs; the BVs processed to reach the WAC limit with AP-107 was extrapolated to 1010 BVs.

6. The total Cs loaded onto the lead column (0.0402 mmoles Cs/g CST) was about 20% less than those from the simulant testing (0.0497 and 0.0523 mmoles Cs/g CST, Fiskum et al. 2019a) and AP-107 processing (0.0509 mmoles Cs/g CST, Fiskum et al. 2019b) despite the higher number of BVs processed with AP-105DF.

7. The AP-105DF SVs processed to reach the WAC limit as a function of flowrate were evaluated. The AP-105DF generally matched the curve established with AP-107, both veered to lower SVs processed to reach the WAC when compared to the trajectory established by the simulant testing (Fiskum et al. 2019a). This was indicative that other components may be consuming exchange sites, the tank waste matrix itself was limiting Cs loading, or occlusion was occurring.

8. The transition zones for Cs breakthrough were calculated to be 341 BVs (20% to 80% Cs breakthrough range) and 626 BVs (5% to 95% Cs breakthrough range).

6.3 Analyte Fractionation

1. Major components Al, K, Na, P, and S partitioned exclusively to the effluent. Minor component Ca also portioned to the effluent (99% recovery).

2. Approximately 29% of the Pb was found in the effluent; a Pb breakthrough curve was obtained with 50% C/C_0 reached at 260 BVs.

3. Based on stable Sr analysis, 8.9% Sr was recovered in the effluent. Based on ^{90}Sr analysis, only 0.10 % was in the effluent. The ^{90}Sr decontamination factor was 959. A Sr breakthrough curve was measured showing 35% C/C_0 from the lead column after processing 1091 BVs.

4. Most of the U (89%) was found in the effluent composite, indicating partial U removal by the CST from the feed. The U load curve through the lead column indicated a 50% U breakthrough at ~50 BVs.

5. Nb, Ti, and Zr, components of CST (near or below MDL in the feed) were detected in the composite effluent and the selected lead column effluent samples, indicating that CST components were leached into solution. Concentrations of these analytes decreased with

increasing process BVs. Total masses recovered in the 10.9 L composite effluent were small: 0.029 g Nb, ~0.012 g Ti, and ~0.045 g Zr.

6. The effluent contained 18% of the feed Np, 40% of the feed Pu, and 86% of the feed Am. The balances of these isotopes were assumed to remain with the CST. Assuming the retained isotopes were bound only to the lead column CST bed, the CST would contain 77 nCi/g TRU, which is lower than the 100 nCi/g threshold defining TRU waste.

7. The ^{99}Tc (likely anionic pertechnetate) did not significantly exchange onto the CST (93% was recovered in the effluent).

7.0 References

ASME. 2000. *Quality Assurance Requirements for Nuclear Facility Applications*. NQA-1-2000, American Society of Mechanical Engineers, New York, New York.

ASME. 2008. *Quality Assurance Requirements for Nuclear Facility Applications*. NQA-1-2008, American Society of Mechanical Engineers, New York, New York.

ASME. 2009. *Addenda to ASME NQA-1-2008*. NQA-1a-2009, American Society of Mechanical Engineers, New York, New York.

Allred JR, JGH Geeting, AM Westesen, RA Peterson. 2020. *Fiscal Year 2020 Filtration of Hanford Tank Waste 241-AP-105*. PNNL-30485, Rev. 0, RPT-DFTP-021, Rev. 0, Pacific Northwest National Laboratory, Richland, Washington.

Ard KE. 2019. *Specification for the Tank-Side Cesium Removal Demonstration Project (Project TD101)*. RPP-SPEC-61910, Rev. 2. Washington River Protection Solutions, LLC, Richland, Washington.

Bray LA, KJ Carson, RJ Elovich. 1993. *Initial Evaluation of Sandia National Laboratory-Prepared Crystalline Silicotitanates for Cesium Recovery*. PNL-8847, Pacific Northwest Laboratory, Richland, Washington.

Brown GN, LA Bray, CD Carlson, KJ Carson, JR DesChane, RJ Elovich, FV Hoopes, DE Kurath, LL Nenninger, and PK Tanaka. 1996. *Comparison of Organic and Inorganic Ion Exchangers for Removal of Cesium and Strontium from Simulated and Actual Hanford 241-AW-101 DSSF Tank Waste*. PNNL-11120, Pacific Northwest National Laboratory, Richland, Washington.

Buckingham J. 1967. *Waste Management Technical Manual*. ISO-100, Isochem, Incorporated. Richland, Washington.

Fiskum SK, JR Allred, HA Colburn, AM Rovira, MR Smoot, RA Peterson. 2018a. *Multi-Cycle Cesium Ion Exchange Testing Using Spherical Resorcinol-Formaldehyde Resin with Diluted Hanford Tank Waste 241-AP-105*. PNNL-27432, RPT-DFTP-006, Rev. 0, Pacific Northwest National Laboratory, Richland, Washington.

Fiskum SK, HA Colburn, RA Peterson, AM Rovira, and MR Smoot. 2018b. *Cesium Ion Exchange Using Crystalline Silicotitanate with 5.6 M Sodium Simulant*. PNNL-27587, Rev. 0; RPT-DFTP-008, Rev. 0, Pacific Northwest National Laboratory, Richland, Washington.

Fiskum SK, AM Rovira, JR Allred, HA Colburn, MR Smoot, AM Carney, TT Trang-Le, MG Cantaloub, EC Buck, and RA Peterson. 2019a. *Cesium Removal from Tank Waste Simulants Using Crystalline Silicotitanate at 12% and 100% TSCR Bed Heights*. PNNL-28527, Rev. 0; RPT-TCT-001, Rev. 0, Pacific Northwest National Laboratory, Richland, Washington.

Fiskum SK, AM Rovira, HA Colburn, AM Carney, and RA Peterson. 2019b. *Cesium Ion Exchange Testing Using a Three-Column System with Crystalline Silicotitanate and Hanford Tank Waste 241-AP-107*. PNNL-28958, Rev. 0, RPT-DFTP-013, Rev. 0, Pacific Northwest National Laboratory, Richland, Washington.

Fiskum SK, AM Rovira, MG Cantaloub, AM Carney, HA Colburn, RA Peterson, BD Pierson. 2019c. *Impact of Crystalline Silicotitanate Particle Size on Cesium Removal Efficiency*. PNNL-29273, Rev. 0, RPT-DFTP-017, Rev. 0, Pacific Northwest National Laboratory, Richland, Washington.

Fiskum SK, EL Campbell, TT Trang-Le. 2020. *Crystalline Silicotitanate Batch Contact Testing with Ba, Ca, Pb, and Sr*. PNNL-30185, Rev. 0, RPT-DFTP-022, Rev. 0, Pacific Northwest National Laboratory, Richland, Washington.

Hamm LL, T Hang, DJ McCabe, and WD King. 2002. *Preliminary Ion Exchange Modeling for Removal of Cesium from Hanford Waste Using Hydrous Crystalline Silicotitanate Material*. WSRC-TR-2001-00400; SRT-RPP-2001-00134, Westinghouse Savannah River Company, Aiken, South Carolina.

Helfferich F. 1962. *Ion Exchange*. New York, New York, McGraw-Hill Book Company, Inc.

Hendrickson DW, RK Biyani, and MA Beck. 1996. *Hanford Tank Waste Supernatant Cesium Removal Test Report*. WHC-SD-RE-TRP-018, Rev. 0A, Westinghouse Hanford Company, Richland, Washington.

Hougan OA and WR Marshall, Jr. 1947. "Adsorption from a Fluid Stream Flowing Through a Stationary Granular Bed." *Chemical Engineering Progress* 43(4):197-208.

King WD. 2007. *Literature Reviews to Support Ion Exchange Technology Selection for Modular Salt Processing*. WSRC-STI-2007-00609, Washington Savannah Company, Aiken, South Carolina.

Klinkenberg A. 1994. "Numerical Evaluation of Equations Describing Transient Heat and Mass Transfer in Packed Solids." *Industrial and Engineering Chemistry* 40(10):1992.

Pease III LF, SK Fiskum, HA Colburn, and PP Schonewill. 2019. *Cesium Ion Exchange with Crystalline Silicotitanate Literature Review*. PNNL-28343, Pacific Northwest National Laboratory, Richland, Washington.

Rovira AM, SK Fiskum, HA Colburn, JR Allred, MR Smoot, and RA Peterson. 2018. *Cesium Ion Exchange Testing Using Crystalline Silicotitanate with Hanford Tank Waste 241-AP-107.* PNNL-27706, RPT-DFTP-011, Rev. 0, Pacific Northwest National Laboratory, Richland, Washington.

Rovira AM, SK Fiskum, JR Allred, JGH Geeting, HA Colburn, AM Carney, TT Trang-Le, and RA Peterson. 2019. *Dead-End Filtration and Crystalline Silicotitanate Cesium Ion Exchange with Hanford Tank Waste AW-102.* PNNL-28783, Rev. 0; RPT-TCT-003, Rev. 0, Pacific Northwest National Laboratory. Richland, Washington.

Russell RL, PP Schonewill, and CA Burns. 2017. *Simulant Development for LAWPS Testing*. PNNL-26165, Rev. 0; RPT-LPIST-001, Rev. 0, Pacific Northwest National Laboratory, Richland, Washington.

Siewert J. 2019. *Tank Side Cesium Removal (TSCR) IXC-150 Sizing*. RPP-CALC-62497 Rev. 2, Washington River Protection Solutions, Richland, Washington.

Walker Jr. JF, PA Taylor, RL Cummins, BS Evans, SD Heath, JD Hewitt, RD Hunt, HL Jennings, JA Kilby, DD Dee, S Lewis-Lambert, SA Richardson, and RF Utrera. 1998. *Cesium Removal Demonstration Utilizing Crystalline Silicotitanate Sorbent for Processing Melton Valley Storage Tank Supernate: Final Report*. ORNL/TM-13503, Oak Ridge National Laboratory, Oak Ridge, Tennessee.

Westesen AM, SK Fiskum, TT Trang-Le, AM Carney, RA Peterson. 2020. *Small to Full Height Scale Comparisons of Cesium Ion Exchange Performance with Crystalline Silicotitanate*. PNNL-30142, RPT-DFTP-019 Rev. 0, Pacific Northwest National Laboratory. Richland, Washington.

Appendix A – Column Load Data

The AP-105DF lead, lag, and polish column loading raw data are provided in Table A.1. The feed displacement, water rinse, and final fluid expulsion raw data are provided in Table A.2. The raw data include the processed bed volumes (BVs) and corresponding ^{137}Cs concentration in the collected sample, % C/C_0, and the decontamination factor (DF).

Table A.1. Lead, Lag, and Polish Column Cs Breakthrough Results with AP-105DF

Lead Column				Lag Column				Polish Column			
BV	µCi ^{137}Cs/ mL	% C/C$_0$	DF	BV	µCi ^{137}Cs/ mL	% C/C$_0$	DF	BV	µCi ^{137}Cs/ mL	% C/C$_0$	DF
12	1.20E-5	9.86E-6	1.01E+7	42	4.77E-5	3.92E-5	2.55E+6	598	3.11E-4	2.56E-4	3.91E+5
42*	2.97E-5	2.44E-5	4.09E+6	84	3.41E-5	2.80E-5	3.57E+6	644	4.91E-4	4.03E-4	2.48E+5
62	9.98E-5	8.20E-5	1.22E+6	127	2.89E-5	2.38E-5	4.21E+6	687	4.78E-4	3.93E-4	2.55E+5
85*	7.60E-4	6.24E-4	1.60E+5	170	2.24E-5	1.84E-5	5.43E+6	730	1.66E-3	1.36E-3	7.35E+4
105	3.70E-3	3.04E-3	3.29E+4	221	7.07E-5	5.81E-5	1.72E+6	774	4.84E-3	3.97E-3	2.52E+4
128*	1.37E-2	1.13E-2	8.88E+3	264	1.78E-4	1.46E-4	6.84E+5	822	1.23E-2	1.01E-2	9.88E+3
146	4.33E-2	3.55E-2	2.81E+3	300	7.04E-4	5.78E-4	1.73E+5	865	2.92E-2	2.40E-2	4.16E+3
172*	1.24E-1	1.02E-1	9.79E+2	343	7.50E-4	6.16E-4	1.62E+5	903	6.06E-2	4.98E-2	2.01E+3
192	2.58E-1	2.12E-1	4.73E+2	386	3.05E-3	2.50E-3	3.99E+4	945	1.08E-1	8.88E-2	1.13E+3
223*	6.59E-1	5.41E-1	1.85E+2	429	1.06E-2	8.74E-3	1.14E+4	965	1.77E-1	1.45E-1	6.90E+2
266	1.85E+0	1.52E+0	6.59E+1	471	3.11E-2	2.56E-2	3.91E+3	1009	3.52E-1	2.89E-1	3.46E+2
303*	3.50E+0	2.88E+0	3.48E+1	491	5.32E-2	4.37E-2	2.29E+3	1033	4.64E-1	3.81E-1	2.63E+2
346	6.71E+0	5.51E+0	1.81E+1	520	9.25E-2	7.60E-2	1.32E+3	1052	6.14E-1	5.05E-1	1.98E+2
389*	1.13E+1	9.31E+0	1.07E+1	566	2.36E-1	1.94E-1	5.17E+2	1076	7.96E-1	6.54E-1	1.53E+2
432	1.76E+1	1.44E+1	6.93E+0	604	4.48E-1	3.68E-1	2.72E+2				
495*	2.82E+1	2.32E+1	4.31E+0	651	9.40E-1	7.72E-1	1.30E+2				
523	3.35E+1	2.75E+1	3.64E+0	694	1.69E+0	1.39E+0	7.21E+1				
570	4.32E+1	3.55E+1	2.82E+0	737	2.95E+0	2.42E+0	4.13E+1				
608	5.33E+1	4.38E+1	2.28E+0	781	4.55E+0	3.74E+0	2.67E+1				
655	6.20E+1	5.09E+1	1.96E+0	829	7.08E+0	5.81E+0	1.72E+1				
698	6.86E+1	5.63E+1	1.78E+0	872	9.67E+0	7.95E+0	1.26E+1				
741*	7.76E+1	6.37E+1	1.57E+0	911	1.33E+1	1.09E+1	9.17E+0				
834	9.13E+1	7.50E+1	1.33E+0	954	1.71E+1	1.40E+1	7.13E+0				
916	9.93E+1	8.16E+1	1.23E+0	996	2.22E+1	1.82E+1	5.49E+0				
1002	1.08E+2	8.85E+1	1.13E+0	1041	2.86E+1	2.35E+1	4.26E+0				
1091*	1.12E+2	9.21E+1	1.09E+0	1085	3.40E+1	2.80E+1	3.58E+0				

BV = bed volume, 10 mL/BV
DF = decontamination factor
C_0 = 122 µCi ^{137}Cs/ mL (reference date June 2020)
* = samples submitted for additional analysis to assess selected constituent breakthrough profiles

Table A.2. Feed Displacement, Water Rinse, and Final Fluid Flush Results Following AP-105DF Processing

Feed Displacement					Water Rinse				Final Fluid Flush			
BV	Density (g/mL)	µCi ^{137}Cs/ mL	% C/C$_0$	DF	BV	µCi ^{137}Cs/ mL	% C/C$_0$	DF	BV	µCi ^{137}Cs/ mL	% C/C$_0$	DF
1.8	1.29	8.42E-1	6.91E-1	1.45E+2	2.0	1.51E-2	1.24E-2	8.06E+3	5.2	1.73E-1	1.42E-1	7.03E+2
3.6	1.29	8.80E-1	7.23E-1	1.38E+2	3.9	1.25E-2	1.02E-2	9.77E+3				
5.4	1.30	9.22E-1	7.58E-1	1.32E+2	5.7	1.72E-2	1.41E-2	7.09E+3				
7.1	1.28	8.57E-1	7.04E-1	1.42E+2	7.5	2.32E-2	1.91E-2	5.24E+3				
8.9	1.13	2.54E-1	2.09E-1	4.79E+2	9.3	2.55E-2	2.10E-2	4.77E+3				
10.8	1.05	4.55E-2	3.74E-2	2.68E+3	11.2	2.22E-2	1.82E-2	5.49E+3				

BV = bed volume, 10 mL
DF = decontamination factor
C$_0$ = 122 µCi ^{137}Cs/ mL (reference date June 2020)
Densities of water rinse samples and final fluid flush were ~1.02 g/mL

Appendix B – Analyte Concentrations as a Function of Loading

The load behaviors of selected analytes in AP-105DF were evaluated from selected samples collected from the lead column. Analysis results of these samples are summarized in Table B.1.

Table B.1. Analyte Concentrations of Selected Samples from the Lead Column During AP-105DF Processing

BV Processed>	NA	42	85	128	172	223	303	389	495	741	1091
Sample ID>	TI082-Comp-Feed	TI082-L-F2-A	TI082-L-F4-A	TI082-L-F6-A	TI082-L-F8-A	TI082-L-F10-A	TI082-L-F12-A	TI082-L-F14-A	TI082-L-F16-A	TI082-L-F22-A	TI082-L-F26-A
Analyte	ICP-OES, M										
Al	5.26E-1	5.04E-1	4.97E-1	5.37E-1	5.11E-1	5.49E-1	5.11E-1	5.45E-1	5.19E-1	5.26E-1	5.08E-1
Ca	1.03E-3	9.08E-4	7.93E-4	9.91E-4	8.28E-4	9.56E-4	8.08E-4	1.02E-3	1.03E-3	1.06E-3	1.06E-3
Cd	[2.4E-5]	[1.4E-5]	[2.2E-5]	[2.0E-5]	[1.4E-5]	[2.2E-5]	[2.4E-5]	[3.7E-5]	[2.5E-5]	[2.1E-5]	[2.1E-5]
Fe	[2.0E-5]	<1.6E-5	<1.6E-5	[2.9E-5]	<1.6E-5	[1.7E-5]	[2.1E-5]	[3.6E-5]	[2.0E-5]	[3.2E-5]	[1.8E-5]
K	1.02E-1	1.01E-1	9.90E-2	1.03E-1	1.02E-1	1.06E-1	9.82E-2	1.05E-1	1.01E-1	1.02E-1	9.80E-2
Ti	<5.9E-6	[2.0E-5]	[1.8E-5]	[1.7E-5]	[1.6E-5]	[1.6E-5]	[1.3E-5]	[2.1E-5]	[1.1E-5]	[1.1E-5]	[1.1E-5]
Zr	<9.4E-6	[4.7E-5]	[4.5E-5]	[4.6E-5]	[3.7E-5]	[4.2E-5]	[3.8E-5]	[3.9E-5]	[3.4E-5]	[2.7E-5]	[2.4E-5]
Analyte	ICP-MS, M										
Ba	<1.6E-6	<2.6E-6	<1.4E-6	<1.4E-6	<1.4E-6	<1.8E-6	<1.5E-6	<1.3E-6	<1.9E-6	<2.0E-6	<3.4E-6
Nb	2.74E-7	4.50E-5	2.92E-5	2.29E-5	1.82E-5	1.54E-5	1.27E-5	1.24E-5	1.06E-5	8.77E-6	6.16E-6
Pb	9.00E-5	5.12E-6	7.05E-6	1.24E-5	1.86E-5	3.12E-5	5.80E-5	7.73E-5	8.37E-5	8.91E-5	9.30E-5
Sr	1.82E-6	6.85E-7	6.54E-7	2.15E-7	2.21E-7	2.32E-7	2.17E-7	2.32E-7	2.78E-7	4.15E-7	7.59E-7
^{238}U	2.46E-5	1.05E-5	1.92E-5	2.34E-5	2.26E-5	2.43E-5	2.48E-5	2.75E-5	2.64E-5	2.76E-5	2.74E-5
Analyte	Radiochemistry, µCi/mL[(a)]										
^{90}Sr	6.90E-01	3.91E-04	5.24E-04	1.14E-03	2.03E-03	3.98E-03	8.72E-03	1.58E-02	3.62E-02	9.34E-02	2.41E-01
^{237}Np	6.69E-06	1.04E-06	1.62E-06	2.46E-06	2.54E-06	3.22E-06	3.12E-06	3.56E-06	4.36E-06	4.62E-06	5.16E-06
^{238}Pu	6.37E-06	4.13E-06	4.56E-06	6.25E-06	3.96E-06	4.67E-06	5.81E-06	4.20E-06	3.27E-06	2.47E-06	3.87E-06
$^{239+240}$Pu	3.94E-05	1.58E-05	2.03E-05	2.03E-05	1.77E-05	2.25E-05	2.28E-05	2.16E-05	2.08E-05	2.08E-05	2.38E-05

(a) Reference date is December 2020.
BV = bed volume, 10 mL
Bracketed values indicate the associated sample results were less than the estimated quantitation limit but greater than or equal to the MDL. Analytical uncertainties for these analytes are > ±15%.
Additional analyte concentrations may be found in Appendix C, ASR 1097.

Appendix C – Analytical Reports

Analytical reports provided by the Analytical Support Operations (ASO) are included in this appendix. In addition to the analyte results, they define the procedures used for chemical separations and analysis, as well as quality control sample results, observations during analysis, and overall estimated uncertainties. The analyses are grouped according to Analytical Service Request (ASR) number. Cross reference of ASO sample IDs to test description are provided in the body of the report (see Table 3.2 and Table 3.6).

Appendix C Table of Contents

Pacific Northwest National Laboratory

902 Battelle Boulevard
P.O. Box 999
Richland, WA 99354
1-888-375-PNNL (7665)

www.pnnl.gov